Progress in Polymer Science 112 (2021) 101324

Contents lists available at ScienceDirect

Progress in Polymer Science

journal homepage: www.elsevier.com/locate/progpolymsci

# Methyl cellulose solutions and gels: fibril formation and gelation properties

McKenzie L. Coughlin[a,1], Lucy Liberman[a,1], S. Piril Ertem[b], Jerrick Edmund[a], Frank S. Bates[a,*], Timothy P. Lodge[a,b,**]

[a] Department of Chemical Engineering & Materials Science, University of Minnesota, Minneapolis, MN 55455, USA
[b] Department of Chemistry, University of Minnesota, Minneapolis, MN 55455, USA

ARTICLE INFO

*Article history:*
Received 19 August 2020
Revised 13 November 2020
Accepted 15 November 2020
Available online 18 November 2020

*Keywords:*
Methylcellulose
Gelation
Fibril
LCST

ABSTRACT

Methyl cellulose (MC) is a semiflexible cellulose ether derivative with a wide range of industrial applications, owing to its water solubility at low temperatures and thermoreversible gelation upon heating. The gelation mechanism of aqueous MC solutions has been debated for many years. However, in 2010, gelation was discovered to be concurrent with fibril formation upon heating, whereby the MC polymer chains self-assemble into fibrils with a remarkably consistent mean diameter, largely independent of polymer concentration, molecular weight, and temperature of gelation. This discovery has shed important light on the gelation mechanism, and initiated studies that lead to more intriguing questions about the fibrils themselves. This review emphasizes various developments since the discovery of fibril formation, while highlighting unanswered questions that require further investigation.



*Abbreviations*

| | |
|---|---|
| 1D | one dimensional |
| 2D | two dimensional |
| 3D | three dimensional |
| $a$ | unit cell dimension |
| $A_2$ | second virial coefficient |
| AGU | anhydroglucose unit |
| $b$ | unit cell dimension |
| $c$ | unit cell dimension parallel to fiber axis |
| $\chi$ | Flory-Huggins interaction parameter |
| CMC | carboxymethyl cellulose |
| cryo-TEM | cryogenic transmission electron microscopy |
| De | Deborah number |
| DS | degree of substitution |
| $DS_{OH}$ | hydroxyl content after methyl substitution |
| DSC | differential scanning calorimetry |
| EC | ethyl cellulose |
| EHEC | ethyl (hydroxyethyl) cellulose |
| $\gamma$ | monoclinic unit cell angle |
| $G'$ | storage modulus |
| $G''$ | loss modulus |
| $\|G^*\|$ | complex modulus |
| GA | glutaraldehyde |
| GRAS | Generally Recognized As Safe |
| HPMC | hydroxypropyl methyl cellulose |
| HPMCAS | hydroxypropyl methyl cellulose acetate succinate |
| HPC | hydroxypropyl cellulose |
| $I$ | intensity |
| $\lambda$ | wavelength |
| $l_p$ | persistence length |
| LCST | lower critical solution temperature |
| $M$ | molecular weight |
| MAXS | mid-angle X-ray scattering |
| MC | methyl cellulose |
| MS | molar substitution |
| $N$ | volumetric degree of polymerization |
| $NaBPh_4$ | sodium tetraphenylborate |
| NMR | nuclear magnetic resonance |
| PEG | poly(ethylene glycol) |
| PEI | polyethyleneimine |
| $\varphi$ | volume fraction |
| $\phi_e$ | equilibrium volume fraction |
| PNIPAm | poly(*N*-isopropyl acrylamide) |
| $q$ | modulus of the scattering wavevector |
| $S$ | number of chains in a junction |
| SANS | small-angle neutron scattering |

* Corresponding author at: Department of Chemical Engineering & Materials Science, University of Minnesota, Minneapolis, MN 55455, USA.
** Corresponding author at: Department of Chemistry, University of Minnesota, Minneapolis, MN 55455, USA.
*E-mail addresses:* bates001@umn.edu (F.S. Bates), lodge@umn.edu (T.P. Lodge).
[1] These authors contributed equally to this work.

https://doi.org/10.1016/j.progpolymsci.2020.101324
0079-6700/

| | |
|---|---|
| SAOS | small-amplitude oscillatory shear |
| SAXS | small-angle X-ray scattering |
| $\sigma^*$ | critical shear stress |
| $T$ | temperature |
| $T_{gel}$ | gelation temperature |
| $T_\theta$ | theta temperature |
| $T_{sol}$ | dissolution temperature |
| $\theta$ | scattering angle |
| WAXS | wide-angle X-ray scattering |
| *xfib*-MC | methyl cellulose fibrillar gel crosslinked at 80 °C |
| *xsol*-MC | methyl cellulose gel crosslinked at room temperature |
| $\zeta$ | number of chain segments in a junction |

## 1. Introduction

Methyl cellulose (MC) is a common cellulose ether derivative that is considered 'Generally Recognized As Safe (GRAS)' by the U.S. Food and Drug Administration [1]. MC is produced commercially through partial functionalization of the cellulose backbone with methyl groups. This process typically involves swelling solid cellulose in a highly basic solution then reacting it with halogenated alkanes such as methyl chloride to convert a fraction of the hydroxyl groups on the anhydroglucose repeat units (AGU) to methoxy groups [2,3]. The average number of positions substituted per monosaccharide is called the degree of substitution (DS). As the DS ranges from 0 (unsubstituted cellulose) to 3 (fully substituted, assuming no end-group effects), there are eight possible repeat unit structures for MC, as shown in Fig. 1. The highly heterogeneous reaction leads to compositional variance (and thus a variable DS) along the backbone, due to the amorphous regions of cellulose chains being more susceptible to methylation than crystalline ones. Commercial MC typically has a DS of 1.7–2.2, producing a semiflexible polymer that is water soluble at low temperatures, due to the disruption of intra- and inter-chain hydrogen bonding in cellulose [4,5]. Other processes have been developed to produce a more homogeneously substituted MC, using various cellulose-selective solvents or a multi-stage addition process of methylation [6,7]. Another possibility is to regio-selectively substitute methyl groups onto the C2, C3, or C6 positions of the cellulose AGUs using protecting groups such as thexyldimethylchlorosilane to selectively protect one, two, or three of the hydroxyl groups [8]. The water compatibility of MC, as well as its status as GRAS, enables use in a wide variety of applications, including pharmaceutical products, foods, ceramics and construction materials, and in cosmetic and personal care products, typically as a thickener, binder, emulsifier, coating, and/or stabilizer [7,9]. This wide commercial usage of MC provides great incentive for a deeper understanding of its solution behavior. Furthermore, MC in a solution is a semiflexible chain, the properties of which have been a topic of great interest to Professor G. C. Berry. As this review will highlight, both rheological and scattering characterization of MC are essential tools for unlocking its fascinating behavior. Professor Berry has been both a pioneer and a world expert in these techniques, and the corresponding authors have benefited greatly from his advice and encouragement over many years.

Upon heating, MC displays lower critical solution temperature (LCST) behavior and undergoes intermolecular association to form a turbid gel [4,10–14]. This thermoreversible gelation is evidenced by sharp increases (over multiple orders of magnitude) in both the storage modulus ($G'$), particularly, and also the loss modulus ($G''$) [4,5,12–22]. The temperature at which this transition from solution to gel occurs ($T_{gel}$), and the gel strength, are tunable depending on the heating rate [12], MC molecular weight [20–22], and concentration of the precursor solution [4,12,14,18]. $T_{gel}$ increases with heating rate, as seen in Fig. 2a [12]. Upon cooling, there is significant hysteresis before the sample reaches a temperature where the gel returns to its original solution state ($T_{sol}$). Interestingly, the dissolution process is relatively independent of the cooling rate, and the modulus remains relatively constant at 80 °C for all rates [12]. The strength of the gel does increase, however, with increasing concentration, as shown by McAllister et al. [18] and in Fig. 2b. For increasing concentration, there is an increase in the complex modulus, $|G^*|$, at all temperatures, along with a decrease in $T_{gel}$ at a given heating rate. Arvidson et al. [12] showed that the gel modulus scales approximately as $\varphi^{2.3}$, where $\varphi$ is the volume fraction of MC. The gel modulus can also be tuned to some extent through the molecular weight. Schmidt et al. [22] demonstrated that $G'$ increases with increasing $M$, although the $T_{gel}$ remains constant. Additionally, it has been shown that when MC has a more regular substitution pattern at constant DS, $T_{gel}$ is reduced and the gel strength increases [5,6]. Determination of the substitution pattern can be difficult, although the mole fractions of the un-, mono-, di-, and tri-substituted AGUs have been quantified through a combination of hydrolysis of the polymer chains and chromatography to separate the fragments [23,24] or through $^{13}$C-NMR spectroscopy [7,25–27]. Additionally, Kono et al. [28] used $^{13}$C-NMR spectroscopy to determine the distribution of the eight possible AGUs for both commercial MC and samples synthesized

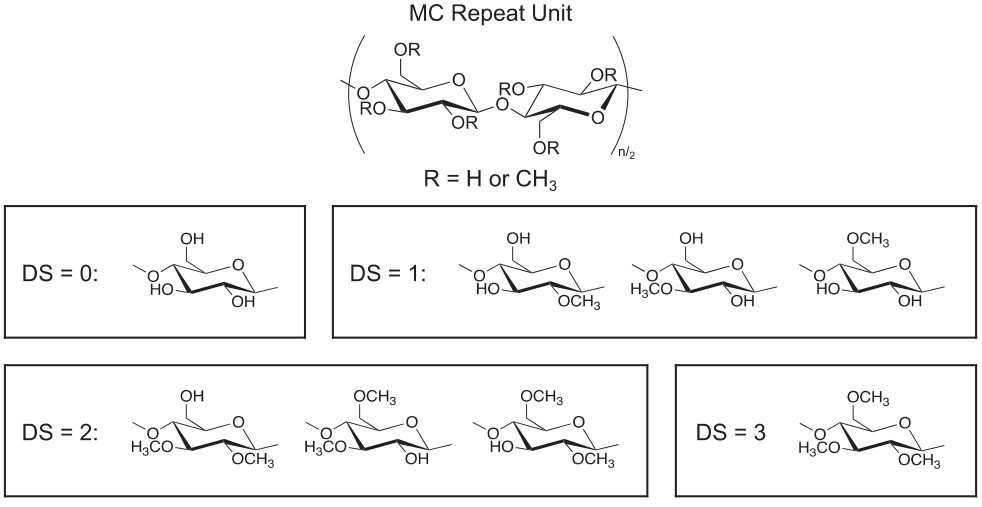


**Fig. 1.** The repeat unit structure of MC with linkages is shown (top). The eight possible structures formed by methyl substitution of the AGU in MC are also included.

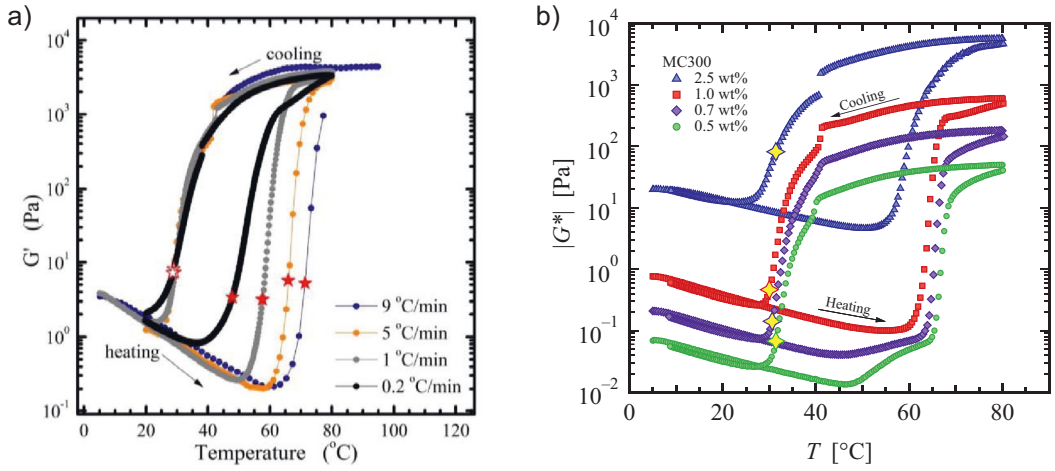


**Fig. 2.** Thermoreversible gelation of MC. (a) Gelation temperature increases with heating rate, but the modulus at 80 °C and $T_{sol}$ remain constant. The orange stars indicate the cross-over points between $G'$ and $G''$, i.e., $T_{gel}$ on heating and $T_{sol}$ on cooling [12], Copyright 2012. Reproduced with permission from the American Chemical Society. (b) Gel strength depends on concentration of MC in solution. Complex modulus, $|G^*|$, increases with increasing concentration, and $T_{gel}$ decreases. The yellow stars mark $T_{sol}$ as the cross-over points between $G'$ and $G''$ [18], Copyright 2015. Reproduced with permission from the American Chemical Society.

with DS ranging from 0.66 to 2.41. To investigate the effect of DS on gelation, Desbrières et al. [25] synthesized MC with homogeneous methyl group substitution with DS ~ 0.9 to 2.2, and found that without the presence of tri-substituted AGUs, MC did not gel, thereby underscoring the importance of a distribution of methyl group substitution for MC gelation. Sarkar [29] also found that both the gel strength and rate of gelation of MC increase with methyl content

## 2. Mechanisms of gelation

Although MC has been studied and commercially produced for over a century [2,3], the mechanism of MC gelation at elevated temperatures has historically been controversial. Prior to 2012, various proposed mechanisms of gelation included physical crosslinking [4,16,30,31], micelle formation [9,10,26,32,33], and kinetically trapped phase separation [11,13–15,25,27,34,35]. From the results of X-ray diffraction experiments on MC, Kato et al. [30] attributed gelation to the tri-substituted AGUs that act as crystalline crosslinks of the gel network. Previous NMR studies have shown that, on average, MC has ~ 20–27% AGUs with tri-substituted methyl groups [7,23,24,28,36,37]. The formation of crystals, proposed to act as crosslinks in the gel state, was confirmed by Khomutov et al. [31]. Haque and Morris [4] proposed that gelation is due to hydrophobic association of regions of dense methyl substitution, and that residual cellulosic domains are also involved in crosslinking. The proposed mechanism involved a two-step process where MC chains are held in "bundles" at low temperature due to unsubstituted cellulose regions, and as the temperature is raised, some of these bundles become hydrated, allowing the methylated repeat units to be exposed to water. Then as the temperature is raised further, the hydrophobic strands attached to different bundles associate to form crosslinks in the gel. This two-step mechanism where MC chains are in "bundles" inherently assumes that MC does not form a true molecular solution at low temperature. This assumption was invalidated by McAllister et al. [18], where static light scattering showed that MC forms individual semiflexible coils in dilute solution at room temperature. Hydrophobic crosslinking of MC was illustrated in cartoon form by Li et al. [16] (Fig. 3a), and was attributed to the increase in hydrophobicity and dehydration of the methoxy groups upon heating that cause the formation of aggregates.

Some researchers also suggested that micelles constituted the junction points in the MC gel. The gel structure for MC was proposed by Rees [32] to be due to the formation of "fringed micelles" consisting of highly methylated AGUs associated by hydrophobic interaction. Sarkar [9] agreed with this interpretation and described the "micellar gels" as analogous to those found in nonionic surfactants, where the micelles are liquid-like in the core. Ibbett et al. [26] found using $^{13}$C-NMR spectroscopy that there is a range of hydrophobicity along the backbone due to the heterogeneous methyl substitution. This causes the chains to adopt a micelle configuration upon heating, which is followed by phase separation such that the phase-separated domains are held in place by the micelles. Takahashi et al. [10,33] described MC gelation behavior using the modified Eldridge-Ferry theory developed by Tanaka et al. [38-41], where associating polymers form multichain junctions upon gelation, as illustrated in Fig. 3b. The junction shape in MC gels was proposed to be fringed-micellar crystallites with 2–4 chains in the micelle [33].

Another commonly proposed mechanism for gelation is viscoelastic phase separation. In this process, the lower critical solution temperature (LCST) behavior of MC leads to kinetically trapped, interconnected polymer-rich domains during phase separation that are held in place through polymer entanglements. The gel point would then be reached when the polymer-rich domain spans the entire sample. A cartoon for the process of gelation through viscoelastic phase separation was illustrated by Tanaka [42] (Fig. 3c). Some researchers suggested that phase-separation-induced gelation in MC is a multi-step process [11,14,15,25,27]. For example, Chevillard and Axelos [11] reported that MC can form three different gels in the phase diagram. At both low and high concentration, a clear gel forms, from associated hydrophobic domains and from crystallites, respectively. At high temperatures, gelation is due to phase separation where polymer-rich microdomains prevent bulk phase separation and result in a turbid gel. Hirrien et al. [27] studied how the distribution of methyl moieties affects gelation and conducted measurements that supported the three-gel phase diagram proposed by Chevillard and Axelos. In contrast, Arvidson et al. [12] showed that when rheological and cloud point measurements were made at the same heating rate, the gel point and the cloud point were coincident, over a very wide range of concentrations. Desbrières et al. [15,25] concluded that gelation was due to phase separation from hydrophobic association. Kobayashi et al. [14] described gelation as a two-step

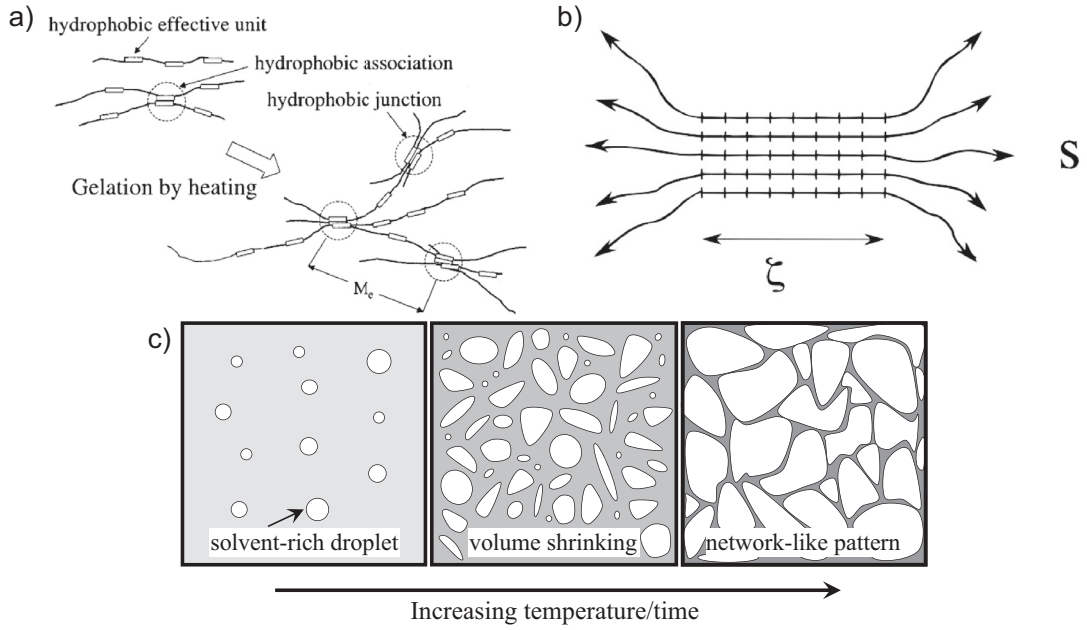


**Fig. 3.** Older models of MC gelation. (a) Crosslinking mechanism of gelation due to association of hydrophobic domains [16], Copyright 2001. Reproduced with permission from the American Chemical Society. (b) Mechanism of gelation proposed by Rees [32] and described theoretically by Tanaka et al. [38–41], where the junction points are micelles formed by associating polymers. Polymers can form junctions made up of $S$ chains and $\zeta$ segments of each chain [40], Copyright 1996. Reproduced with permission from the American Chemical Society. (c) Viscoelastic phase separation mechanism where polymer-rich domains (gray) coarsen upon heating and become kinetically trapped. Figure drawn based on an illustration from reference [42].

process where the hydrophobic regions along the backbones associate, followed by phase-separation-induced gelation that is held in place by the aggregates between chains. More recently, Fairclough et al. [13] observed the phase separation process using optical microscopy and concluded that phase separation of MC led to a bicontinuous structure via spinodal decomposition. Using small-angle light scattering experiments, Villetti et al. [35] also concluded that the phase separation occurs through spinodal decomposition leading to a bicontinuous network. However, this study relied on jumps from low to high temperature instead of a temperature ramp, which could have affected the results because the gelation temperature is heating-rate dependent, as mentioned previously.

## 3. Fibril formation

### 3.1. Experimental observations

Direct experimental imaging of MC solutions and gels, corroborated by indirect information, changed the established perception related to the gelation mechanism and opened interesting fundamental new questions. Cryogenic transmission electron microscopy (cryo-TEM) of dilute MC solutions revealed that gelation is concurrent with the self-assembly of MC chains into long fibrils, which percolate into a strong network upon heating [22,43–45]. Fig. 4 presents a representative series of cryo-TEM images taken upon heating 0.2 wt% MC solutions, showing the formation of MC fibrils in the vicinity (55 °C), at (60 °C), and above (65 °C) the rheologically-determined gelation temperature. The fibrillar structure has been confirmed and further quantified by small-angle neutron and X-ray scattering (SANS and SAXS) [22,44,45]. Both SANS and SAXS profiles of MC solutions exhibit a characteristic shoulder in the scattering curve (intensity $I$ versus modulus of the scattering wavevector $q = 4\pi\lambda^{-1}\sin(\theta/2)$, where $\lambda$ is the radiation wavelength and $\theta$ is the scattering angle), which develops upon heating to slightly below and then above the gelation temperature,

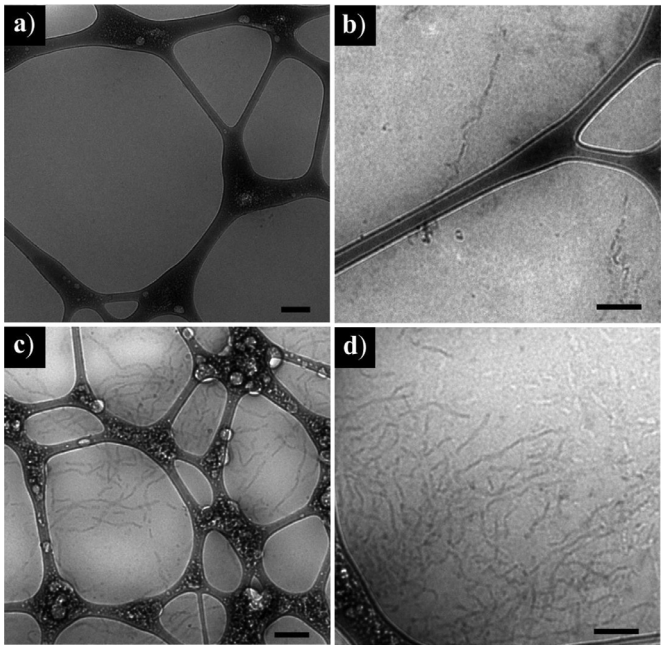


**Fig. 4.** Cryo-TEM of 0.2 wt% solutions of 300 kg/mol MC annealed for 30 min at (a) 50 °C, (b) 55 °C, (c) 60 °C, (d) 65 °C before vitrification. The formation of fibrils occurs upon heating. The dark network in the images corresponds to the lacey carbon support of the TEM grids. Scale bars are 200 nm [44], Copyright 2013. Reproduced with permission from the American Chemical Society.

characteristic of structure formation in the system (Fig. 5). A semiflexible cylinder model with disperse radii consistently describes the SAXS and SANS data well [46,47]. Measurements of the fibril diameter from cryo-TEM images, and fitting of the SANS/SAXS data to the semiflexible cylinder model, result in a remarkably consistent mean fibrillar diameter of ~15–20 nm [22,44,45]. Moreover, the fibrillar structure and diameter were shown to be system-

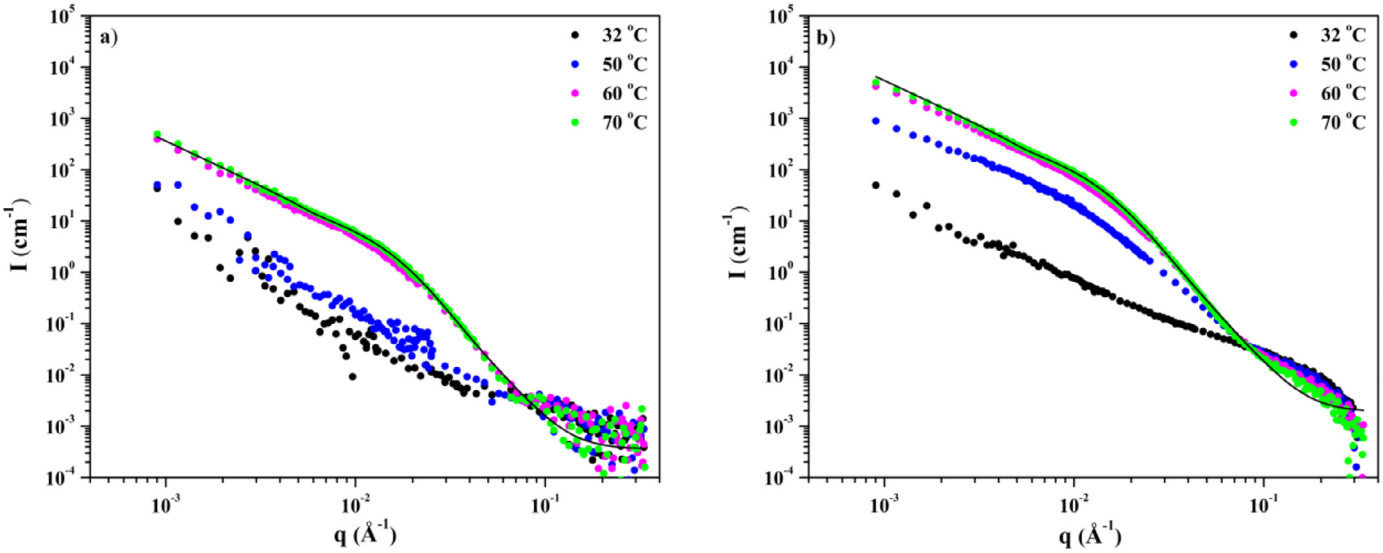


**Fig. 5.** SANS data for (a) 0.09 wt % and (b) 1.3 wt % 300 kg/mol MC solutions in $D_2O$. Gelation temperatures are 63 °C and 50 °C, respectively [12]. The black lines are best fits to the scattering curves at 70 °C. Above the gel point, a shoulder indicating fibril formation appears near $q \approx 0.02$ Å$^{-1}$ [44], Copyright 2013. Reproduced with permission from the American Chemical Society.

atically independent of MC concentration, MC molecular weight, temperature of gelation, and the regiochemical distribution of the methyl moieties [22,45].

The discovery of the fibrils motivated researchers to understand MC gelation in the context of fibril formation and understand the structure and formation of the fibrils. Extensive cryo-TEM studies revealed that the well-established hysteresis seen in rheology measurements is dominated by fibril formation upon heating, and fibril dissolution upon cooling [12,45]. Assuming that all the polymer chains are incorporated into fibrils at high temperatures, SANS measurements and fitting of the absolute intensity scattering data revealed that the fibrils consist of ~ 60% by volume of water [45].

Schmidt et al. [22] combined rheology, SAXS, and cryo-TEM experiments to explore the effect of MC molecular weight on the fibrillar structures and gelation. Rheology measurements of 0.3 wt% solutions at 80 °C showed a monotonic increase of the gel modulus with molecular weight. Fitting of the SAXS traces for the different molecular weight samples resulted in a constant mean fibril diameter, regardless of the molecular weight. In general, the length of the fibrils was too large to be determined by SANS or SAXS. However, complimentary cryo-TEM results showed that lower molecular weight solutions were characterized by shorter fibrils (Fig. 6), which induced a less connected gel network with a lower degree of crosslinking, providing a plausible explanation for the lower gel modulus. This work suggests that fibrils percolate into a gel network through crosslinks, but the precise origin of the crosslinks is still unknown. The authors also proposed that the length of the shorter fibrils is determined by the contour length (molecular weight) of the MC chains that are presumably oriented along the fibril axis [22].

These recent experimental findings shed light on the intermolecular association that underlies the rheological behavior of MC solutions and gels, yet at the same time raise puzzling questions. How do such heterogeneous polymers self-assemble into reproducible fibrillar structures upon heating, irrespective of their concentration, molecular weight, temperature of gelation, and distribution of the methyl substitutions along the polymer chains? Furthermore, what is the self-assembly mechanism, and what factor(s) are responsible for the relatively uniform diameter?

Simulations of MC fibril formation with a toroidal structural motif predict that the diameter of the fibrils is mainly controlled by the Kuhn length of the polymer chains, which collapse into toroid structures that are then stacked together into fibrils [48–52]. However, the experimental study by Schmidt et al. [22] suggests that MC chains are organized in twisted bundles, as modeled by Hall et al. for generic semiflexible chains [53], where the diameter is controlled by the helical pitch of the chains. The helical pitch is presumed to be determined by the elasticity/Kuhn length of the chains, with the interchain interactions mediated by water molecules. More recent experimental work by Schmidt et al. [54] focused on the substructure of the fibrils, revealed by combining phase-plate cryo-TEM with small-, mid-, and wide-angle X-ray scattering (SAXS, MAXS, and WAXS, respectively), leading to the conclusion that the fibril structure is more complex than initially thought or suggested by molecular simulation. The results of this study indicate that the fibrils are constructed from small diameter (ca. 10 nm), denser semicrystalline regions, and “ghost”-like regions with larger diameter (ca. 26 nm), characterized by very low contrast in phase plate cryo-TEM, and invisible in regular cryo-TEM (Fig. 7). The small diameter regions were assumed to contain polymer chains that are oriented along the fibril axis, and the larger diameter sections were attributed to swollen, amorphous polymer chain bundles. The authors suggest that nucleation of the ordered, semicrystalline regions might set the overall average diameter of the fibrils [54].

The precise self-assembly mechanism of the MC chains into fibrils and the source of the reproducible fibril diameter awaits further investigations and should be addressed by additional experimental approaches.

### 3.2. Models of fibrils

Recently, there has been an increase in computational efforts aimed at providing insight into the fibril structure as well as the mechanism of fibril formation. There are several ways in which self-attractive polymers such as MC could aggregate to form a fibrillar structure. Given that MC is a derivative of cellulose, one possible structure is the stacking of chains in a parallel configuration, similar to what is seen in cellulose fibrils [30,43]. However, such axial chain stacking does not provide a mechanism for stabilizing a specific finite fibril radius as seen in experiments. Structures that could result in a uniform radius include collapsed toroids that

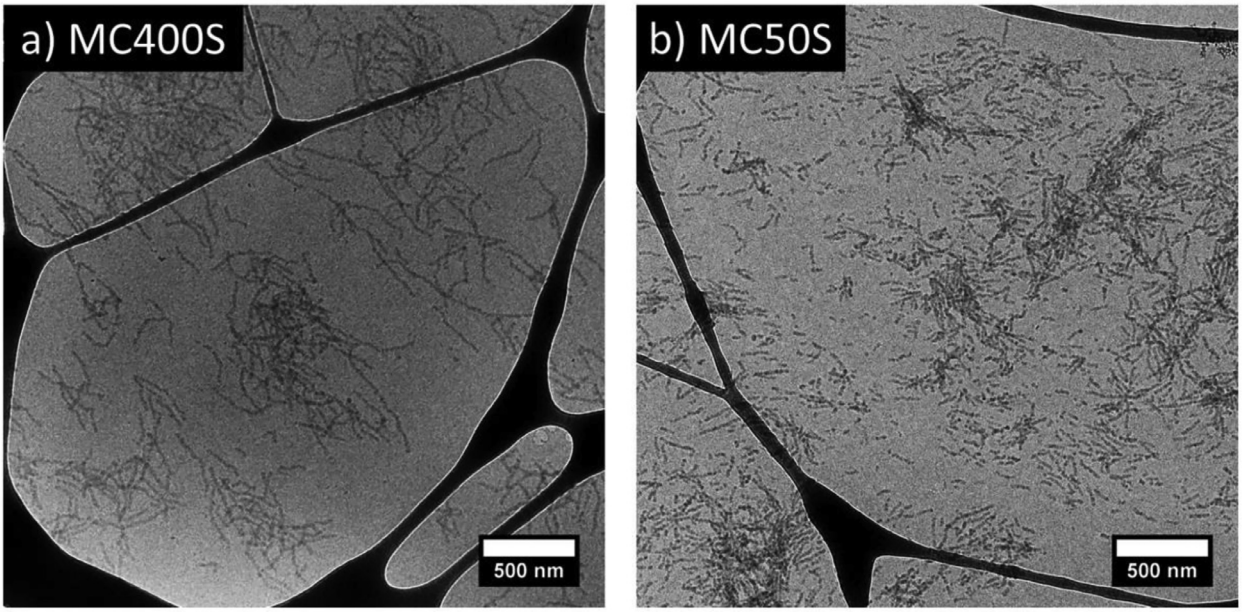


**Fig. 6.** Cryo-TEM of 0.1 wt % MC fibrillar solutions, characterized by MC molecular weight of (a) 400 kg/mol (b) 50 kg/mol. The solutions were annealed at 80 °C for 30 min. The specimen characterized by lower molecular weight MC shows the formation of shorter fibrils. The dark network in the images corresponds to the lacey carbon support of the TEM grids [22], Copyright 2018. Reproduced with permission from the American Chemical Society.

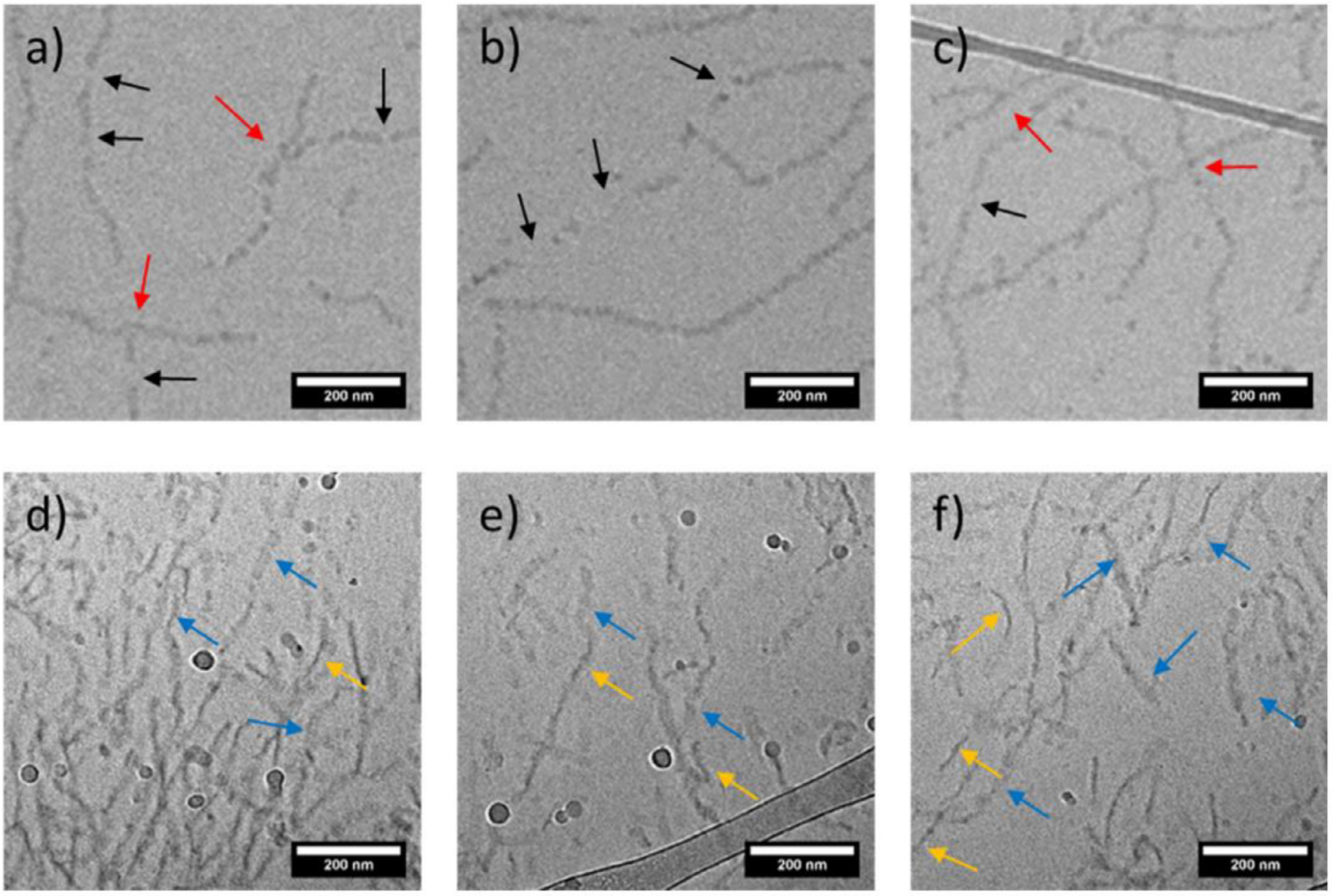


**Fig. 7.** Cryo-TEM of MC fibrils. (a-c) Cryo-TEM images of 0.2 wt% 300 kg/mol MC showing "ghost"-like (black arrows) regions and branching points (red arrows). (d-f) Phase-plate cryo-TEM of 0.05 wt % 150 kg/mol MC revealing low contrast/density regions (blue arrows) and darker, higher density regions (orange arrows) [54], Copyright 2020. Reproduced with permission from the American Chemical Society.

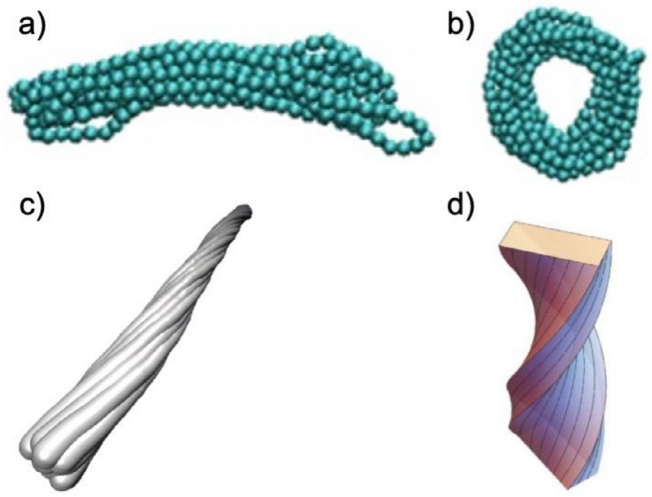


**Fig. 8.** Models of fibril structures include (a) chain stacking [49], Copyright 2016. Adapted with permission from Multidisciplinary Digital Publishing Institute, (b) toroid model [49], Copyright 2016. Adapted with permission from Multidisciplinary Digital Publishing Institute, (c) twisted bundles [56], Copyright 2018. Adapted with permission from Multidisciplinary Digital Publishing Institute, and (d) helical tapes [58], Copyright 2017. Adapted with permission from the Royal Society.

stack together coaxially [48–52], twisted rope-like bundles [22,54–57], and folded helical tapes (Fig. 8) [53,58]. Huang et al. [49] have shown that as self-attractiveness increases, isolated semi-flexible chains collapse into rings, where the radius of the ring is set by the persistence length ($l_p$) of the macromolecule. Recent simulations have extended this to MC and have shown that the polymer chains can assemble into toroidal structures that ultimately stack into fibrils at elevated temperatures [48,50–52]. Huang et al. [48] used coarse-grained molecular dynamics to show that isolated MC chains with over ca. 600 monomers collapse into toroids at higher temperatures. Ginzburg et al. [50] have determined that with increasing temperature MC chains undergo a transition from coils to rings, assuming that the molecular weight is large enough. The rings have an outer diameter ranging from 14 to 17 nm, which agrees well with experimental observations [18,22,44,45,54,55]. However, this outer diameter limits the smallest MC chain length that can form fibrils. Since the walls of the torus consist of more than one layer of polymer chain, the predicted minimum limit is 25–30 kg/mol for a chain to form one full cycle around a toroid [50]. This is in contrast to recent experimental work showing that MC chains with a weight average molecular weight of 22 kg/mol form fibrils upon heating, with no decrease in the overall chain conversion to fibrils [22]. Additionally, the hollow center of the toroidal ring could account for the 60% water content in the fibrils, though the void fraction determined through simulations ranges from only 13% to 26% [48,50]. To explain the low void fraction from only considering the hollow center, Ginzburg et al. [50] estimated that each spherical bead representing a monomer contains about 45% of polymeric material by volume, which in turn yields 52% total void space in the toroid structure, much closer to the experimental value.

While there is no direct experimental evidence for toroidal rings, simulation studies have shown that they could be a precursor to fibrils [50–52]. Ginzburg et al. [50] proposed that the rings stack on top of each other to form fibrils. They used systems containing two to fifteen MC chains to simulate the precursor steps for fibril formation. Individual rings were set in multiple initial configurations, and the results showed that the rings fused together to form a single “proto-fibril”. Additionally, when multiple proto-fibrils were placed near each other, they combined to form a larger tube structure. The results suggest that the ring stacking could result in long fibrils with Y-junctions as potential branch points that can act as crosslinks in high concentration to form a fibrillar network. Additionally, the simulated elastic modulus of the proto-fibrils increased with the concentration of the rings, consistent with experimental observations. This ring stacking mechanism assumes that the rings are inherently stable within the proto-fibril. However, other simulations have shown that the toroidal structure is not static in nature and could be metastable [51,52]. A time-resolved simulation study by Li et al. [51] showed that the toroids undergo rapid conformational fluctuations. They found that the rings formed at 50 °C will change shape many times during a simulation to form bifocal structures, as well as a “splayed” configuration before re-forming a ring shape. Additionally, individual rings in a proto-fibril undergo rapid conformational fluctuations that allow the chain to come into contact with another ring or proto-fibril and ultimately drag the second ring back to itself to form a single fibrillar structure. A further study by Sethuraman and Dorfman [52] found that the mechanism for fibril formation depends on the initial distance between the chains. When rings are initially close together, ring stacking is observed, as predicted by Ginzburg et al. [50]. Furthermore, all chains in these stacks of rings undergo rapid conformational fluctuations. The outer rings in the stack exhibit the largest fluctuations, indicating that fibril formation is more likely to occur in the axial direction to form long fibrils, as seen experimentally [18,22]. Fluctuations of the central rings could be a source of branching. As the initial distance between the rings increases, chains will form bifocal structures, collapsed states, and even isolated rings. These structures form fibrils due to rapid conformational fluctuations instead of through ring stacking. Sethuraman and Dorfman [52] simulated a mixture of rings and random chains to investigate the assumption of a two-stage fibril formation mechanism, whereby chains first collapse into rings then come together to form fibrils. In this simulation, both the random chains and the ring structures undergo rapid conformational fluctuations and can “reach out” to capture other chains, suggesting that the ring structure is likely metastable. Overall, the results support a ring nucleation mechanism for fibril formation, instead of ring stacking. The fact that the SAXS/MAXS/WAXS shows alignment of MC chains with the fibril axis effectively rules out any ring stacking mechanism.

These studies on the toroid model can account for some of the observations, but recent experimental results have shown that there is a relationship between fibril length and contour length of MC chains [22] that has yet to be accounted for computationally. With this correlation in mind, another possible fibril structure is axially oriented MC chains twisted into a rope-like bundle, as shown by Vargas-Lara and Douglas for a fiber network in semiflexible polymer solutions [56]. In this model, the MC chains would stack together, and the local chirality of the anhydroglucose unit would cause the chains to twist as they bundle together. This has been shown previously for cellulose nanofibrils [59]. The amount of twist in the chain increases radially from the center of the bundle. Grason et al. have shown that this type of assembly is constrained by the inherent chirality of the filaments, with the radius of the bundle being set by the persistence length of the filaments [53,58,60–62]. The radius of the bundle increases as $(l_p d)^{1/2}$, where $d$ is the planar distance between filaments. This scaling law was confirmed experimentally by Morozova et al. [55] though it has not been specifically studied computationally for MC. All recent experimental evidence should be considered by supplementary computational modelling efforts, which will be of great importance for targeting and resolving the remaining open questions regarding the self-assembly mechanism.

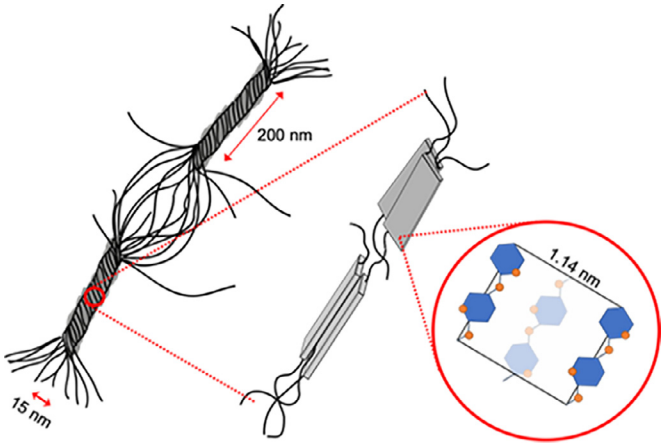


**Fig. 9.** Schematic depiction of the proposed heterogeneous fibrillar structure composed of semicrystalline and amorphous regions [54], Copyright 2020. Reproduced with permission from the American Chemical Society.

### 3.3. Internal structure of fibrils

A close examination of MC gels (both wet and dry) through a combination of SAXS, MAXS, and WAXS revealed that the fibrils have a semicrystalline structure (Fig. 9) with ca. 34% crystallinity [54,63]. MAXS and WAXS data suggested that both wet and dried MC gels have distinct peaks at wavevector moduli $q$ = 0.56, 0.93, 1.25, 1.51, and 1.87 Å$^{-1}$, which are broadly consistent with the findings of Kato et al. [30] Dried films were further investigated via MAXS and WAXS after alignment of the fibrils by uniaxial stretching. Reflections were found to be consistent with a two-chain body-centered monoclinic unit cell (four AGUs per unit cell), with dimensions $a$ = 1.14 nm, $b$ = 0.89 nm, and $c$ = 1.02 nm, with angle $\gamma$ ranging from 90 to 100° (Fig. 10 and Fig. 11). The authors noted that the monoclinic angle was not precisely resolved because of absence of angular resolution in the (00$l$) orientation. The $c$ dimension was aligned with the fiber axis and was exactly equal to the length of two AGU units [64–66]. This result confirms that on average the MC chain axis is aligned with the fibrils, effectively ruling out the toroidal model.

It is now established that the fibrillar internal structure is partially constructed of semicrystalline regions, and that MC gelation is concomitant with formation of a network of fibrils. However, the polymer crystalline fraction and the self-assembly mechanism of the polymer chains into fibrils are still unknown, and require further investigation. Two alternative self-assembly mechanisms have been proposed to account for the partial crystallinity [54]. One possibility is that MC self-assembly is initialized by nucleation of the semicrystalline regions, followed by association and growth of the fibrils, as depicted in Fig. 12. This mechanism would limit the fibril diameter based on restrictions over the nucleus size due to congestion created by packing of amorphous hydrated sections of polymer around the ordered region. Another option is phase separation and coalescence of the chains into hydrated fibrils, followed by crystallization due to association of the more hydrophobic regions. The coincident development of the shoulder in SAXS patterns (Fig. 13a), the MAXS/WAXS peaks (Fig. 13b), and the simultaneous growth of the integrated intensity of the SAXS patterns and WAXS peak (Fig. 14), favor the first proposed mechanism.

### 3.4. Puzzling thermodynamic behavior

The discovery of MC self-assembly into fibrils encouraged researchers to understand the dilute solution phase behavior of MC upon heating. McAllister et al. [18] explored MC in dilute solution

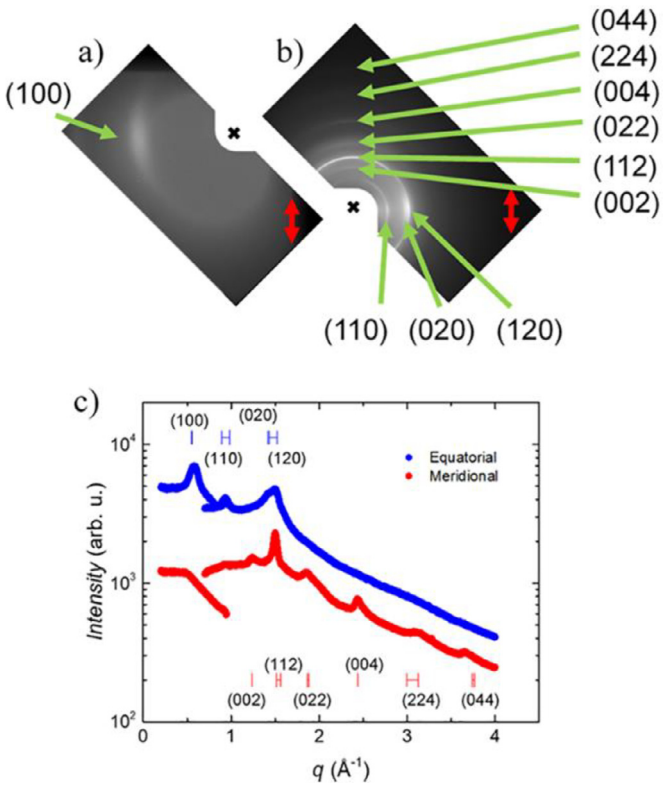


**Fig. 10.** MAXS and WAXS data of dried and stretched MC films and peak indexing of the monoclinic unit cell. (a) 2D MAXS exhibits an anisotropic reflection perpendicular to the fibril axis, assigned as (100). (b) 2D WAXS features higher-order peaks along the fibril axis, with a first peak assigned as (002). The rest of the peaks are consistent with a monoclinic unit cell with dimensions of $a$ = 1.14 nm, $b$ = 0.89 nm, and $c$ = 1.02 nm, and an angular range of $\gamma$ = 90–100°. (c) 1D MAXS and WAXS data with the peak indexing [54], Copyright 2020. Reproduced with permission from the American Chemical Society.

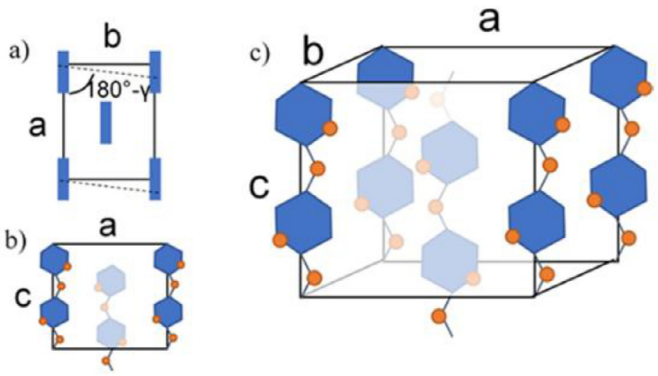


**Fig. 11.** Schematic illustration of the proposed unit cell with dimensions $a$ = 1.14 nm, $b$ = 0.89 nm, and $c$ = 1.02 nm, with $\gamma$ in the range of 90–100°. (a) In-plane view of the unit cell. The dashed line indicates the possible range of the monoclinic angle. (b) Length-axis view of the unit cell. The central chain is assumed to be oriented parallel to the rest of the chains. (c) 3D view of the proposed monoclinic unit cell [54], Copyright 2020. Reproduced with permission from the American Chemical Society.

by light scattering, cryo-TEM, and rheology. Static light scattering showed a seemingly "classical" LCST behavior, with a theta temperature $T_\theta \approx$ 48 °C, and a positive second virial coefficient ($A_2$) at $T < T_\theta$. Nevertheless, light scattering from dilute solutions annealed for longer periods of time (ca. days to weeks) below 48 °C indicated that aggregation of MC can still occur. Moreover, cryo-TEM of solutions near the overlap concentration, annealed at 40 °C for 3 weeks, reveal self-assembly of the polymer chains into indi-

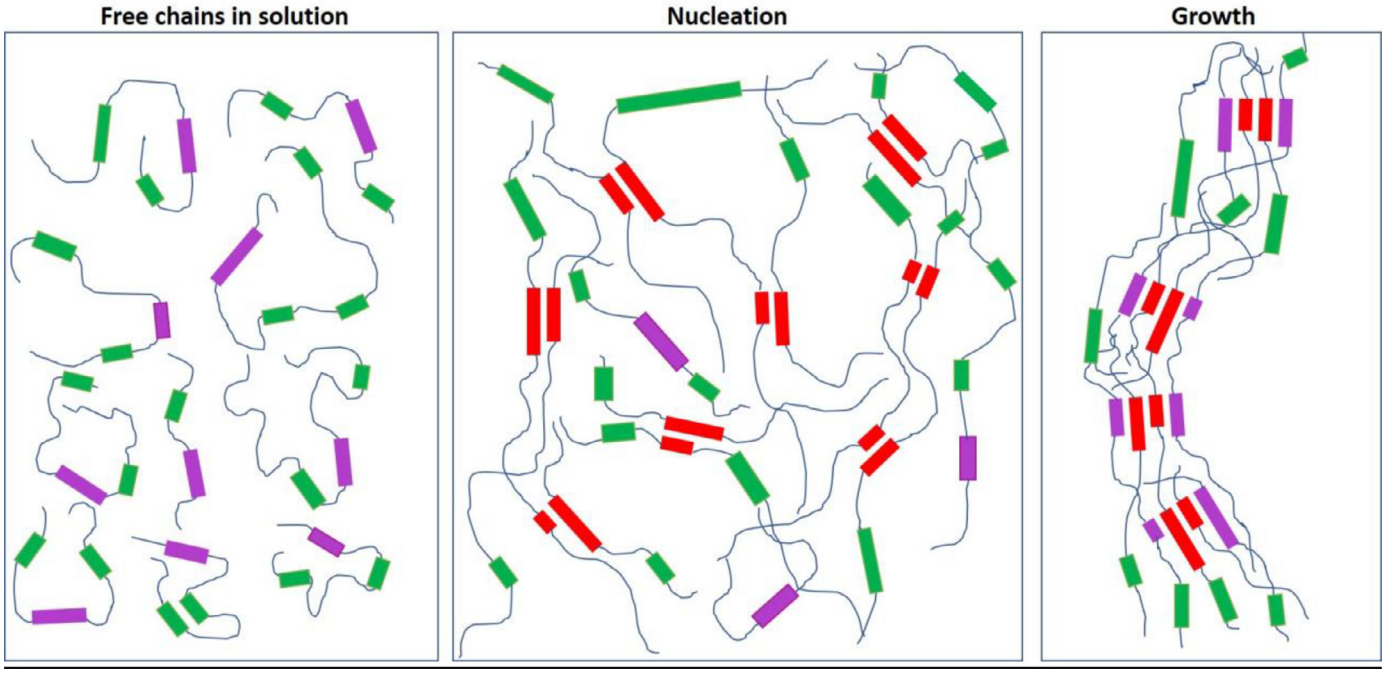


**Fig. 12.** Schematic representation of the suggested nucleation and growth mechanism of MC fibrils. Purple indicates preferentially tri-methylated sections (~ 25% of the chain) of the MC chain that can participate in the crystallization process (34%). Green corresponds to AGU sections with fewer methyl groups that end up in amorphous regions. Red is to highlight the hydrophobic parts that participate in the nucleation process, where the nuclei are constructed of 2 chains.

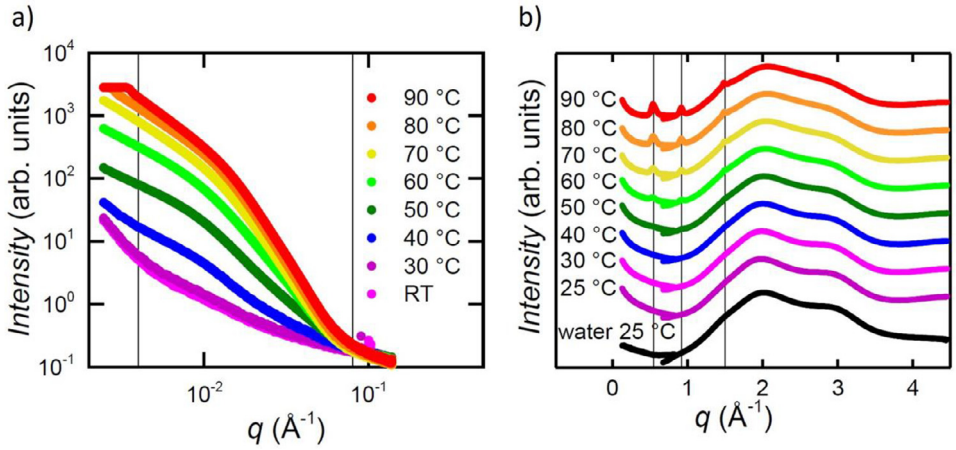


**Fig. 13.** (a) SAXS and (b) MAXS/WAXS of a 7 wt% 300 kg/mol MC solution as a function of temperature [63], Copyright 2018. Reproduced with permission from University of Minnesota Digital Conservancy.

vidual fibrils, structurally similar to fibrils formed upon gelation at higher concentrations. The aggregation and association of the MC polymer chains into fibrils, under what appear to be good solvent conditions, raises intriguing questions. How is fibril formation possible below the LCST temperature, where the second virial coefficient is positive? What is the equilibrium state of the system?8??

According to Flory-Huggins theory, the phase behavior of a polymer solution is mainly dictated by the interaction parameter $\chi$, and by the volumetric degree of polymerization $N$. When $\chi$ exceeds 1/2, a flexible coil solution should phase separate at a critical volume fraction, ~ $1/\sqrt{N}$ ($N >> 1$) into a concentrated isotropic phase of overlapping chains in equilibrium with a low concentration phase of collapsed globules [67]. However, for dilute MC solutions, aggregation takes place below the theta temperature, where water is considered a good solvent, which conflicts with the theory. This behavior suggests that isolated MC chains dissolved in water at temperatures below $T_\theta$ are metastable. Rheology experiments imply that the critical temperature for aggregation is 30 °C, where the fibrils consistently dissolve on cooling, independent of rate. Based on the experimental data, the authors [18] proposed that MC behavior resembles that of semiflexible chains, rather than flexible coils, and is governed by phase separation into isotropic and nematic phases. The key parameter is the chain stiffness, or the axial ratio (Kuhn length-to-diameter ratio), following Flory's nematic lattice theory (Fig. 15a) [18,68]. According to this theory, a low concentration of stiff chains can exhibit two-phase equilibrium at temperatures lower than $T_\theta$. Fig. 15b shows a plot of the gel–sol ($T_{sol}$) transition obtained upon cooling, and the sol–gel ($T_{gel}$) transition as found by Arvidson et al. [12] upon slow heating. The solid line in Fig. 15b is the predicted nematic–isotropic binodal estimated for MC chains and was associated with the $T_{sol}$ data. However, the $T_{gel}$ data reflects the metastable region between the two equilibrium limits, and the isotropic–nematic equilibrium limit for the system remains unknown. Moreover, the self-assembly of the

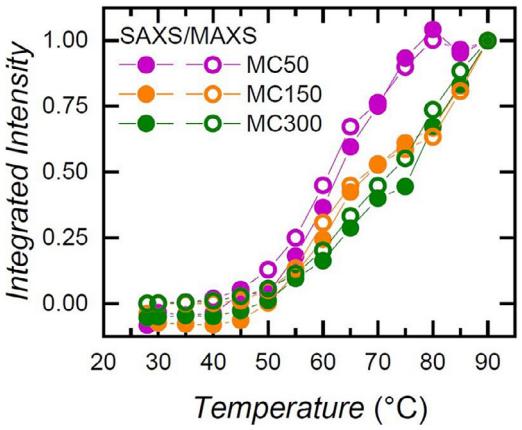


**Fig. 14.** Integrated SAXS and MAXS intensity for MC solutions with molecular weights of 50, 150, and 300 kg/mol. Shows that the conversion from polymer chains to fibrils is concurrent in SAXS and MAXS patterns [54], Copyright 2020. Reproduced with permission from the American Chemical Society.

polymer chains into fibrils with local order [54] rather than macroscopic ordering suggests a kinetically trapped state [18].

### 3.5. Nonlinear rheology

The rheological behavior of fibrillar MC gels has been shown to fit well with existing mechanical models. Large-amplitude oscillatory shear experiments have shown that aqueous MC solutions transition from shear thinning to shear thickening behavior near the gelation temperature, where fibrils are formed. The mechanical response of the resulting gels can be described well by a filament-based mechanical model [69]. The presence of fibrils also increases the shear modulus, consistent with a model developed by MacKintosh et al. [70], which relates the elasticity of individual fibrils to that of the bulk system. Over a wide range of concentrations MC gels have also exhibited a transition from linear to non-linear viscoelastic behavior at a critical shear stress, $\sigma^*$, which is also predicted accurately by the model [69]. Note also that the magnitude of the modulus of an MC gel is well above what would be anticipated for a homogeneous gel of crosslinked chains.

Morozova et al. [71] demonstrated that the addition of salt affects the extensional flow behavior of MC solutions at room temperature. The presence of sodium chloride at high concentration (8 wt%) induces fibril formation at room temperature (discussed below), which changes the mechanical properties. This results in a strong shear-thinning behavior, and elastic flow regimes, whereas the salt-free solution exhibits shear-thinning behavior only at room temperature [71]. This can be reconciled by the Deborah number (De), a dimensionless value of the ratio between the relaxation time and the time of the experiment (time for capillary breakup) which describes viscoelastic behavior. Solutions without fibrils (no salt) are characterized by a low De, and a power-law shear-thinning behavior. However, the formation of fibrils with the addition of salt significantly increases the relaxation time (and De) and the viscosity of the solution. As a result, the fibrillar solution accommodates an elasto-capillary filament thinning behavior, which is a characteristic of elastic fluids. Further work by Micklavzina et al. [72] examined the shear and extensional flow properties of low viscosity MC solutions, at constant temperature of 20 °C, as a function of fibril content, using hyperbolic single phase microfluidic channels. The fibril concentration in solution was controlled by the addition of different NaCl salt concentrations (0–5 wt%). The use of hyperbolic contractions allowed investigations of lower MC molecular weights (150 kg/mol) and higher shear and strain rates, compared to previous rheological studies. Measurements at lower deformation rates (10–100 $s^{-1}$) were shown to agree with previous macroscale rheology studies [71], where higher content of fibrils increases the extensional viscosity. The increase of extensional viscosity was rationalized by polymer alignment in the flow direction. Moreover, at higher deformation rates (100–1000 $s^{-1}$), the MC solutions were demonstrated to undergo extensional thinning behavior. A follow-up study by Metaxas, et al. [73] expanded the previous work [72], and explored previously inaccessible extensional flow properties of lower molecular weight (150 kg/mol) MC solutions with varying NaCl salt concentrations at room temperature, using microfluidic flow-focusing devices. This method, which broadens the range of accessible solution viscosities and extensional strain rates, demonstrated that the flow-driven extensional

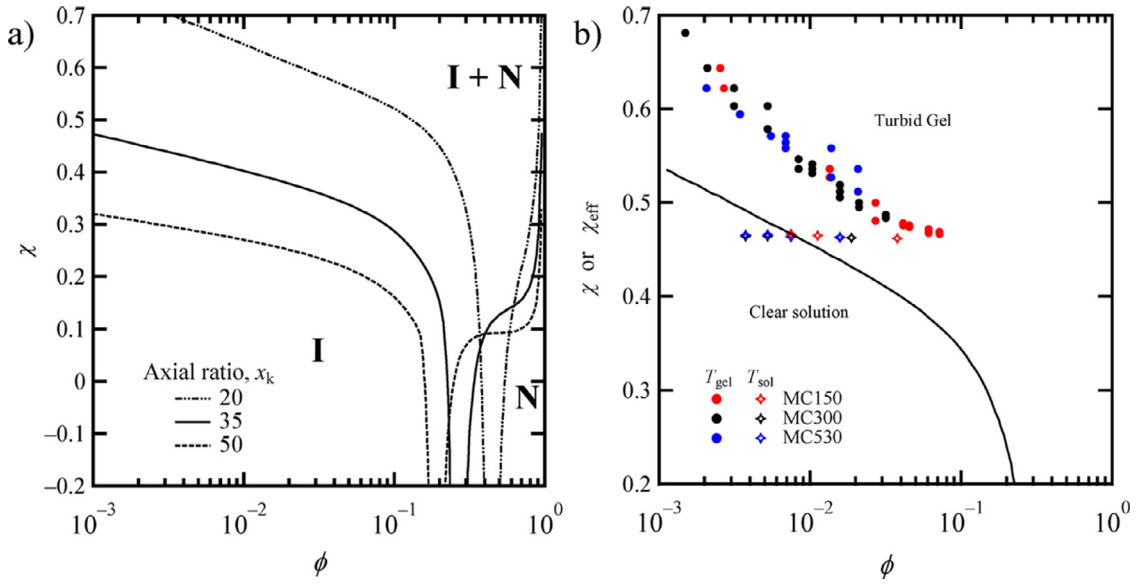


**Fig. 15.** (a) Theoretically predicted isotropic-nematic phase separation curves for semiflexible chains of different axial ratios [68]. (b) Experimentally measured $T_{sol}$ (stars) from Fig. 3 of ref. [18] and $T_{gel}$ (circles) from Arvidson et al. [12] The solid line in (b) corresponds to the predicted binodal line for semiflexible coil of an axial ratio of 28 [18], Copyright 2015. Reproduced with permission from the American Chemical Society.

viscosity of low viscosity MC solutions increases with salt/fibril concentration.

These studies have significantly improved and expanded the understanding of mechanical properties associated with MC solutions, and may open new processing opportunities, such as fiber spinning.

### 3.6. Outstanding issues

The discovery of fibril formation resolved the long-term controversy related to the gelation mechanism of aqueous MC solutions, and substantially improved understanding of structure-property relationships and the mechanical resposne of the system. Nonetheless, this finding raises numerous fundamentally interesting questions.

It is now established that MC exhibits LCST behavior, and upon heating the chains self-assemble into semicrystalline fibrillar structures of ca. 15 nm diameter, while incorporating 60% by volume of water. The internal crystalline structure demonstrates that the polymer chains are oriented along the fibril axis. Moreover, the fibrillar length is closely correlated with the polymer contour length and the gel modulus, and the gelation occurs through percolation of the fibrils into a gel network through crosslinks. However, the exact source of the crosslinks is still unknown.

MC fibrils display peculiar self-assembly behavior. Interestingly, the fibrillar diameter is reproducible and independent of the polymer heterogeneity, concentration in solution, the MC molecular weight, and temperature of gelation. Furthermore, dilute solutions below the LCST temperature (good solvent conditions) show aggregation and association of MC chains into fibrils. This unusual behavior should be addressed by further experimental and computational efforts to understand the self-assembly mechanism, the factors responsible for the remarkably uniform fibril diameter, and to establish the equilibrium state of MC in aqueous media versus what is undoubtedly a non-equilibrium fibrillar gel configuration.

## 4. Modifying gelation

### 4.1. Addition of salt

Over the years, researchers have succeeded in modifying the gelation properties of MC solutions in various ways. Along with advancing the fundamental understanding of these mixtures, a variety of applications, e.g., in food and biological systems, has led to many studies aimed at unraveling the effects of different types of salt on MC solutions.

In 1888, Hofmeister investigated the addition of salts to aqueous protein solutions, and found that the presence of salt affects protein solubility, either enhancing or reducing the apparent hydrophobicity in water [74]. The resulting “Hofmeister series” is a sequence of ions ranked according to their effect on a solute in an aqueous solution. According to the series, a typical ranking for anions is $SO_4^{2-} > S_2O_3^{2-} > H_2PO_4^- > F^- > Cl^- > Br^- >> I^- > SCN^-$, and $Ba^{2+} > Ca^{2+} > Mg^{2+} > Li^+ > Na^+ > K^+$ for cations, where the earlier in the series, the less soluble the protein. A recent publication by Dougherty [75] explains that the addition of salt to water affects the hydrogen bond strength to water molecules; ions earlier in the series interact more strongly with water molecules, tending to induce a “salting-out” effect, which increases the hydrophobicity of a solute in water, and decreases solubility. Ions on the right side are weakly hydrated with water, resulting in a reduction of hydrophobicity and an increase in the solubility of the solute [75]. According to dos Santos et al. [76] the ionic radius plays a role on the extent of interaction of the ions with water. Smaller and higher valency ions have higher surface charge density and are more strongly hydrated by water molecules, which leads to precipitation of the solute. However, large ions have lower charge density and higher polarizability and are weakly hydrated by water, hence larger ions can adsorb to hydrophobic areas of the solute and redistribute their charge towards the water, increasing the solubility of the solute.

Heymann was the first to study the effect of salt addition to MC aqueous solutions [19]. He explored the addition of two groups: chloride salts and potassium salts. By sealing the solutions in a test tube and heating above the gelation temperature, he determined the temperature at which the gel began to flow, and found that the temperature at which the gel reverts back to a solution changes with the addition of different salts in the following order of anions: $SCN^-$, $I^-$, $NO_3^-$, $NO_2^-$, $Br^-$, $Cl^-$, acetate, tartrate, and $SO_4^-$, consistent with the Hofmeister series [74]. Heymann observed that the presence of salting-out salts decreases the gel-to-solution transition temperature, and salting-in salts increase the point of transition. Moreover, according to these results, anions have a much more significant influence than that of cations [19]. In the same manner as the salt effect on the gel-to-solution temperature, the gelation temperature was also shown to be affected by the addition of salt, as reported by Sarkar [9]. This study demonstrated that the addition of an increasing amount of sodium chloride, a salting-out salt, to MC solutions gradually decreased the gelation temperature, and increased the gel mechanical strength. A systematic study by Xu et al. [77] using micro differential scanning calorimetry (DSC) measurements over a variety of salting-in and salting-out salt solutions confirmed that salting-out salts depress the gelation temperature of MC solutions, whereas salting-in salts shift the gelation point to higher temperatures, again in agreement with the Hofmeister series [74]. The gelation temperature was also found to increase or decrease linearly with salt concentration, for salting-in or salting-out salts, respectively [77]. Almeida et al. [78] confirmed by dynamic and steady shear rheological measurements that the gelation temperature linearly decreases with increasing salting-out salt concentration. Another study by Xu et al. [79] investigated the effect of the addition of a mixture of salting-in and salting-out salts to MC solutions. This study showed that the gelation temperature decreases or increases as a function of the salt mixture composition. The relative shift of the gelation temperature was found to be a linear function of the molar ratio between the salts, indicating that the effect of each salt is independent of the other.

The effect of addition of organic salts, such as sodium tetraphenylborate ($NaBPh_4$), to MC solution has also been studied [80,81]. $NaBPh_4$ induces a dual effect as a function of concentration; at low salt concentrations, the gelation temperature decreases, exhibiting a salting-out behavior, and above a critical salt concentration, the gelation temperature increases [80,81]. This interesting transition from salting-out to salting-in can be explained by the attraction of $BPh_4^-$ anions to the MC hydrophobic areas, behaving as a surfactant above the critical salt concentration, thus increasing the MC solubility in water and suppressing the gelation temperature.

The effect of salt on MC gelation has led researchers to explore the impact of salt in terms of fibrils. Liberman et al. [82] investigated the impact of salting-out and salting-in salts on MC fibril formation and structure by small-amplitude oscillatory shear (SAOS) rheology and SAXS. Fig. 16 presents the complex modulus as a function of temperature, for 1 wt% MC solutions with the addition of 0 to 8 wt% of NaCl and NaI [63]. The results show that NaI, a salting-in salt, increases the gelation temperature with increasing salt concentration, and the addition of NaCl, a salting-out salt, decreases the gelation point with concentration, in good agreement with the DSC results previously reported by Xu et al. (Fig. 17) [77].

Liberman et al. [82] were the first to assess the effect of the addition of salt on the morphology of the fibrils. SAXS results on

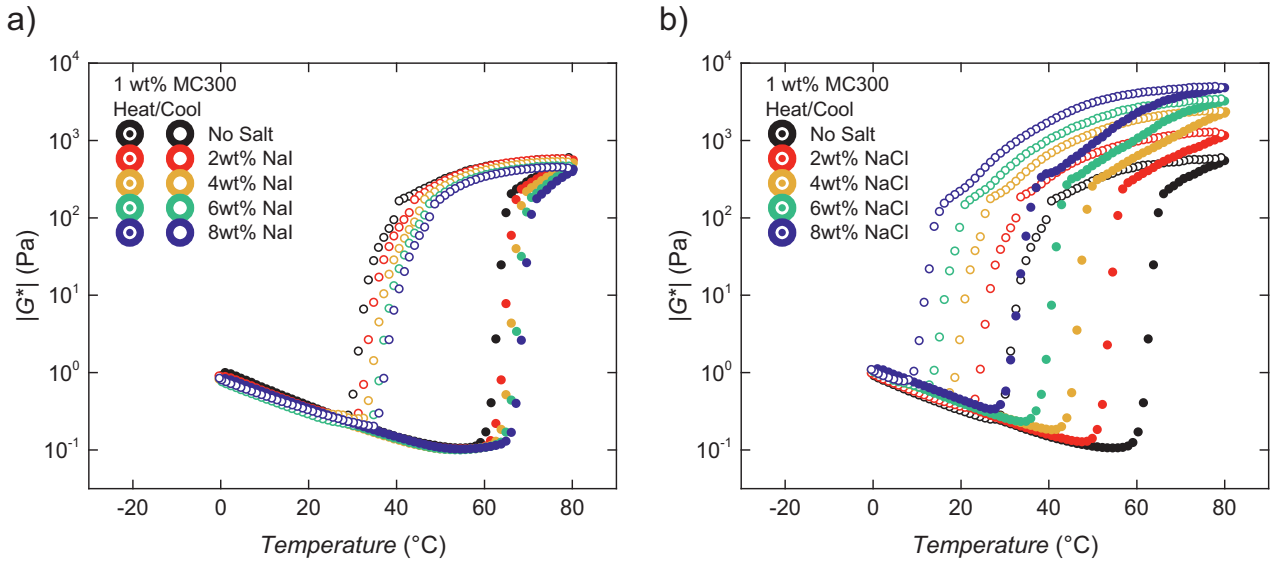


**Fig. 16.** SAOS heating and cooling ramp results for 1 wt% 300 kg/mol MC with the addition of NaI (a) and NaCl (b) at salt concentrations ranging from 0 to 8 wt%. The gelation temperature and the transition from gel to solution increase with NaI concentration and decreases with NaCl. The experiments were conducted at 5% strain, 1 rad/s, and a heating rate of 1 °C/min [63], Copyright 2018. Reproduced with permission from University of Minnesota Digital Conservancy.

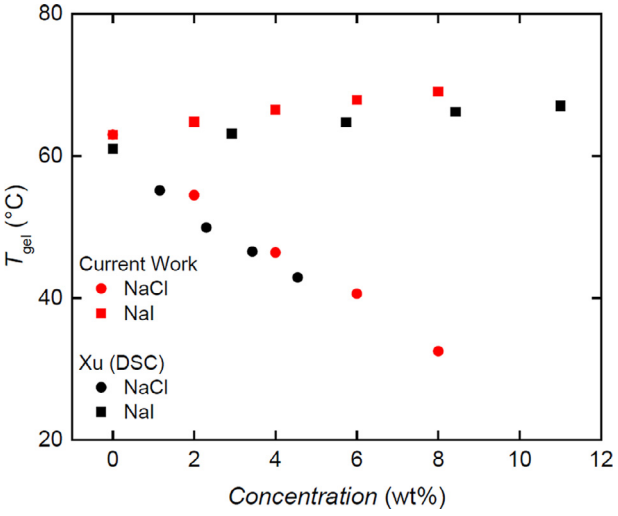


**Fig. 17.** $T_{gel}$ vs. NaI and NaCl salt concentration obtained by Schmidt (red) [63], compared to DSC results by Xu et al. (black) [77]. $T_{gel}$ increases with increasing NaI concentration and decreases with NaCl [63], Copyright 2018. Reproduced with permission from University of Minnesota Digital Conservancy.

salty solutions verified that gelation in the presence of salt is accompanied by fibril formation. Moreover, fitting of the SAXS data to the semiflexible cylinder model has shown that the fibril diameter is mainly dictated by the concentration of the salt, rather than the salt identity, and decreases with salt concentration. However, MAXS and WAXS data obtained from the gels have shown that the internal structure of the fibrils is unaffected by the presence of salt, and is consistent with the data presented in Schmidt et al. [54] for MC fibrils without salt [63]. This means that the diameter reduction primarily reflects the amorphous domains of the fibrils, while the packing of the crystalline areas remains unchanged. However, given that the fibril morphology is unaffected by many other factors, it is still unclear why the diameter decreases with salt concentration. Possible explanations could be dehydration of the fibrils induced by the osmotic pressure caused by the addition of salt, and the effect of the salt on the self-assembly mechanism of the polymer chains into fibrils.

### 4.2. Other cellulose ethers

This section focuses on recent developments with several related cellulosic materials, namely hydroxypropyl methyl cellulose (HPMC), hydroxypropyl cellulose (HPC), ethyl cellulose (EC), ethyl (hydroxyethyl) cellulose (EHEC), and carboxymethyl cellulose (CMC). As with MC, these various cellulose ethers are prepared through the substitution of hydroxyl groups in the 2, 3, and 6 positions around the cellulose ring [83,84]. In addition to sharing typical MC applications, hydroxy-propyl methyl cellulose (HPMC) has found uses ranging from the production of films [85–88] and thermoplastics [89,90], applications in biomedicine [91] and drug delivery [92–98], and in 3D printing [99]. The chemical structure of HPMC is almost identical to MC, with the addition of hydroxypropyl substituents at typical levels (MS) from 0.1 to 0.3 per AGU, and comparative studies of the phase separation and gelation behavior in aqueous solutions are extensive [9,13,29,43,100–107]. Sarkar reported that with increasing HPMC concentration, the gelation temperature systematically decreases, while the cloud point/precipitation temperature decreases in a plateauing fashion, with an intersection at a concentration of 6.5 wt% [9]. Kita et al. found the intersection to be at 11.5 wt% [103]. The gel modulus was found to depend on time, molecular weight, hydroxypropyl group molar substitution (MS), and methyl DS [9,29,102]. In addition, Haque et al. [102] found that HPMC solutions, like MC solutions at low temperature, have shear-thinning properties. A recent paper by Akinosho et al. [106] showed that the relative crystallinity of HPMC decreases with increasing hydroxy-propyl groups. In the thermoreversible gelation of aqueous HPMC solutions upon heating, characteristic sharp drops in $G'$, $G''$, and the complex viscosity are observed first, followed by an increase in $G'$ and crossover with $G''$ that is concurrent with the gelation process, in addition to considerable hysteresis upon cooling [13,29,43,100–105,107]. The first phenomenon is a result of liquid-liquid phase separation that precedes fibril formation, and is not observed in aqueous MC solutions [13,100,104]. In addition, Lodge et al. [100], using similar molecular weights of MC and HPMC, found that the hot gel modulus of HPMC was orders of magnitude lower than that for MC. Bodvik

et al. [101] similarly showed that HPMC solutions at 85–90 °C were orders of magnitude less viscous than MC, and argued that HPMC aggregated more rapidly due to its bulkier substituents. As with MC, the underlying mechanisms of phase separation and gelation of aqueous HPMC solutions is still debated, and numerous explanations recently have been proposed [13,43,100,103,107].

Much like MC, fibril formation in aqueous HPMC solutions upon heating was only discovered over the past decade through a combination of small-angle scattering techniques and cryo-TEM measurements [43,100]. The pioneering work of Bodvik et al. [43] showed that at 65 °C, HPMC with a hydroxypropyl MS of 0.13 formed fibrils in aqueous solutions, albeit less entangled in comparison to MC fibrils. The authors also argued that the presence of hydroxypropyl substituents hinders fibril formation, shifting the development of fibrils to higher temperatures and concentrations [43]. In a recent paper, Lodge et al. [100] found that HPMC with a hydroxypropyl MS of 0.27 formed fibrils at 70 °C that were thicker, shorter, and contained less polymer and were more flexible than MC fibrils. In contrast to these results, Arai et al. [108] reported that MC and HPMC are long and rigid rod particles at room temperature.

Other cellulose ethers such as hydroxypropyl cellulose (HPC), ethyl cellulose (EC), and ethyl (hydroxyethyl) cellulose (EHEC) also show phase separation in aqueous solution, depending on the degrees of substitution of the various groups and the concentration. At low concentration (~ 2 wt%), HPC phase separates, but does not gel in aqueous solution [102,109–111]. For higher concentrations HPC shows an apparent two-step mechanism of phase separation and gelation that is similar to aqueous HPMC solutions [112,113]. EC is soluble in water when the ethoxy DS is between 1.0 and 1.5 [114]. Perhaps its best known property, in comparison to other cellulose ethers, is almost universal solubility in polar and non-polar organic solvents at an ethoxy DS of 2.4–2.5 [114]. The cloud point of aqueous EHEC solutions has been shown to increase with increasing hydroxyethyl DS [109,115]. Bodvik et al. [101] found that EHEC exhibits the fastest aggregation in comparison to HPMC and MC due to its bulky oligo(ethylene oxide) chains. Much like HPMC, EHEC undergoes two critical temperature transitions during the thermal gelation process, with the first transition coinciding with the onset of aggregation and the macroscopic cloud point [101].

CMC is a highly water-soluble anionic cellulose ether that is partially substituted with carboxymethyl groups and commonly used in its acid or sodium salt form (NaCMC). Like MC, aqueous NaCMC solutions exhibit shear-thinning behavior [116]. Although CMC is historically known for its lack of thermal gelation in water [9,109], recent papers have shown that a phase transition does occur in aqueous CMC solutions upon heating [117,118]. To date, none of these various cellulose ethers have been shown to form fibrils upon heating.

### 4.3. Further functionalization of MC

Due to its water solubility and amphiphilic character, MC and its derivatives (e.g., HPMC, HPMCAS, and CMC) have inspired a significant body of research focused on applications in drug delivery [7,92-98]. In order to improve drug-polymer interactions and drug-delivery efficiency, these cellulose ether derivatives are often chemically modified with functional groups. Here we restrict our focus to examples of chemical modification of MC, not only for drug-delivery applications, but also to gain further insight into solution properties and the fiber formation mechanism.

The general approach for chemical modification of MC is to take advantage of the remaining unsubstituted OH functionality ($DS_{OH} = 3 - DS_{CH3}$) and use various reactions to attach functional groups onto the polymer chain. Note that a maximum DS = 3 assumes the MC degree of polymerization is large enough that there is no effect from the end groups. One such modification is the direct conjugation of small molecules to the backbone of MC. Quiñones et al. [119] modified MC through a carbodiimide-mediated cross-coupling reaction between the MC hydroxyl groups with esterified biologically relevant molecules such as testosterone and vitamins D2 and E (Fig. 18a). Attachment of these molecules to MC induced the formation of nanoaggregates in aqueous solution that appeared to be stable dispersions for ca. 1 month. It is also possible to use small molecules that add additional functionality to MC. For example, the Williamson ether synthesis approach can be used to react the hydroxyl groups with alkyl halides, which contain an additional functional group for use in further reactions [55,120-123]. Dong et al. [120] used this method to attach pendant alkenes to the MC backbone, which were further modified using olefin cross-metathesis with acrylic acid and other acrylates. Hydrogenation of the cross-metathesis products enabled the formation of MC derivatives that were able to successfully reduce drug crystallization in solution, thereby expanding potential applications. Dong et al. [121] expanded upon the cross-metathesis approach through thiol-Michael addition to further functionalize the electron-deficient cross-metathesis products with various thiols. Both the cross-metathesis and the thiol-Michael addition reactions are performed under mild conditions, and the combination of the two allows for the synthesis of MC derivatives with diverse structures and tunable functionalities and properties. However, further research is needed to determine how these small molecule architectural modifications affect fibril formation and gelation in MC. The attachment of pendant functional groups using the remaining hydroxyl groups with various techniques has been used to produced crosslinked MC gels, which is discussed in more detail below [122,124-131].

In addition to small molecule addition and crosslinking, some studies have examined backbone modification of MC through grafting of polymers. Kim et al. [132] oxidized MC using sodium periodate, which forms two aldehyde groups on one AGU by cleaving the bond between vicinal carbons with hydroxyl substituents. Subsequently, the aldehyde groups were reacted with 800 g/mol polyethyleneimine (PEI) via reductive amination to produce cationic PEI-grafted MC. The results showed that this method of polymer conjugation actually decreased the MC molecular weight from 35.5 kg/mol to 10.9 kg/mol for PEI-grafted MC, due to the cleavage of MC by over-oxidation. The conjugated polymers were then shown to form stable, spherical polyplexes with plasmid DNA, though the gelation behavior and solution properties of the polymer itself were not examined. Morozova et al. [55,123] used the Williamson ether synthesis approach described above to modify MC with allyl groups, and then systematically conjugated thiol-terminated poly(ethylene glycol) (PEG) to the backbone with photo-initiated thiol-ene click reactions (Fig. 18b). Two PEG molecular weights, 800 g/mol and 2000 g/mol, were used to synthesize polymers with grafting densities ranging from 0.01 to 0.37 PEG grafts/AGU [55,123]. Static and dynamic light scattering results showed that the persistence length ($l_p$) increased systematically with grafting density and that longer PEG grafts had a greater effect than the shorter grafts; these results were in good agreement with a theory by Fredrickson [133]. Additionally, using atomic force microscopy and SAXS, Morozova et al. [55] showed that as $l_p$ increases, the fibrils radius also increases from 10 nm to 16 nm until $l_p$ ~ 23 nm, at which point both gelation and fibril formation are completely suppressed. These results confirm that fibril formation is central to MC gelation. Similar results (unpublished) were obtained by grafting short poly(*N*-isopropyl acrylamide) (PNIPAm) chains to MC, thereby introducing a second LCST moiety. Interestingly, the addition of PNIPAm actually increased the apparent theta temperature, suggestive of unfavorable PNIPAm-MC interactions.

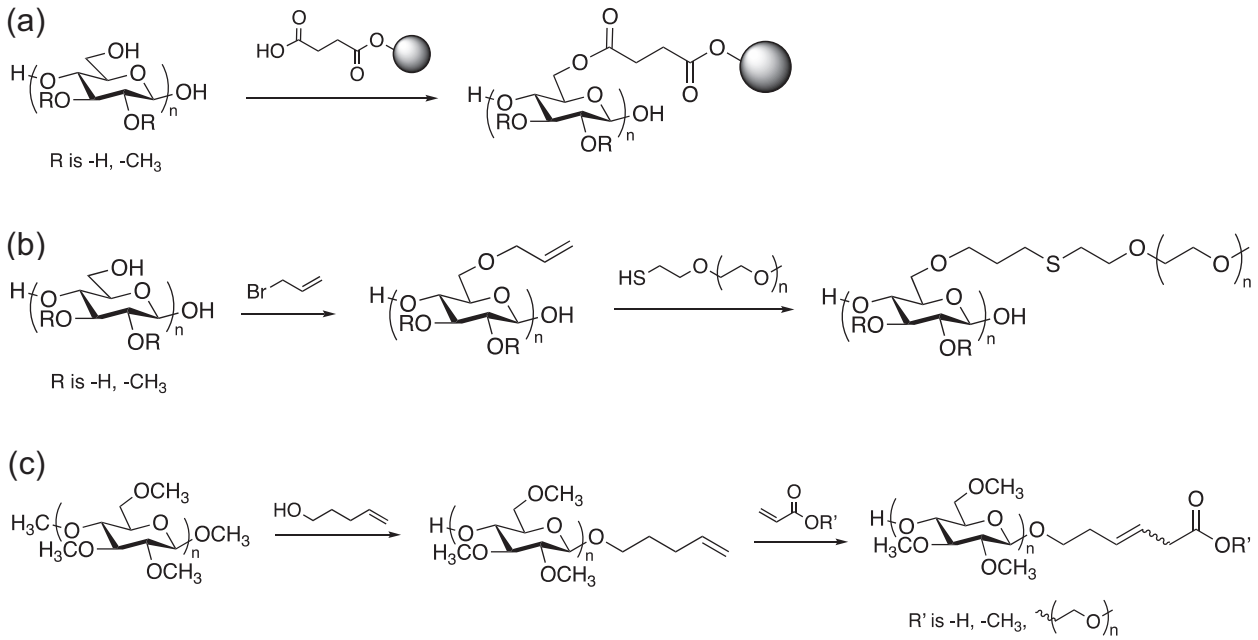


**Fig. 18.** Examples of chemical modification to methyl cellulose. (a) Attachment of small molecules to MC using cross-coupling reaction between unsubstituted hydroxyl groups on the MC backbone and esterified molecules such as testosterone and vitamins D2 and E (gray sphere) [119], Copyright 2019. Adapted with permission from Elsevier Science Ltd. (b) Synthesis of polymer-grafted MC using the Williamson ether synthesis approach to add pendant allyl groups on the MC backbone, followed by thiol-ene click reaction to conjugate PEG to MC [123], Copyright 2017. Adapted with permission from the American Chemical Society (c) Synthesis of MC block copolymers using olefin cross-metathesis of alkene terminated tri-methyl cellulose and acrylate-terminated PEG [147], Copyright 2020. Adapted with permission from Elsevier Science Ltd.

As with any polysaccharide, each MC chain has a reducing end, at which a single AGU is capable of undergoing mutarotation in aqueous solutions through reversible opening of the cyclic hemiacetal into its acyclic form, exposing a single aldehyde group. Using selective chemistries, this aldehyde group can be modified to allow synthesis of MC block copolymers. While many research groups have explored different strategies to form block copolymers from polysaccharides [134–141], there are few examples for MC-derived block copolymers. Early examples by Kamitakahara and coworkers focused on attachment of model compounds to MC enabled by glycosylation of single sugar units [142-145]. One study stands out for developing a synthetic method to introduce a single azide group or a single propargyl group to the reducing and non-reducing ends of tri-methyl cellulose oligomers by performing a Huisgen 1,3-dipolar cycloaddition [146]. Recent work by Chen et al. [147] showed the use of olefin cross-metathesis to conjugate tri-methyl cellulose with poly(ethylene glycol) to form an amphiphilic block copolymer (Fig. 18c) [147]. While the precursor material was MC with DS = 2, the researchers chose to fully methylate MC before conjugation to allow for the possibility of making MC-based triblocks and to have a range of usable reaction conditions due to the enhanced solubility of tri-methyl cellulose in various organic solvents. Future work on synthesizing MC block copolymers could potentially expand the applications for MC, as well as forming interesting self-assembled structures upon heating.

### 4.4. Chemical crosslinking

As MC is derived from the most abundant natural polysaccharide, cellulose, in addition to its unique gelation properties [12], it serves as a promising sustainable material for the preparation of three-dimensional network structures such as hydrogels. MC hydrogels have found applications across the fields of drug delivery [125,127], soft tissue reconstruction [148,149], and tissue engineering scaffolds [124]. However, the thermoreversible nature of aqueous MC solutions renders the MC gels impermanent, as they revert to liquid solutions upon cooling [12]. Since most MC gels are applicable to biological systems between room (25 °C) and body (37 °C) temperatures [124,125,127,148,149], chemical crosslinking of aqueous MC solutions can be used to produce robust hydrogels with tunable material properties at low temperature.

Various reaction mechanisms and pathways have been explored in chemically crosslinking aqueous MC solutions. Urethane linkages using hexamethylene diisocyanate and catalytic dibutyltin dilaurate were used as chemical crosslinkers for MC hydrogel synthesis, by annealing at 70 °C for half an hour [126]. A recent paper by Shin et al. [124] showed that MC hydrogels can be synthesized by the attachment of dicarboxylic acid groups, further modified with tyramine and chemically crosslinked using photosensitive vitamins under visible light. The authors discussed a dual-crosslinking method that involved irreversible photo- and reversible thermal crosslinks, with a maximum temperature studied of 37 °C [124]. Pakulska et al. [125] showed that poly(ethylene glycol)-bismaleimide can be chemically crosslinked with thiol-modified MC within minutes, at physiological pH and room temperature, with no toxic catalysts required. Similarly, the authors explored the effects of both chemical and physical crosslinks on the properties of the MC hydrogel at 37 °C, and showed that the chemically crosslinked MC gels were more stable and swelled less than their physically crosslinked counterparts [125]. In a recent paper by Morozova et al. [122], allyl substituents were first introduced by reacting aqueous MC solutions with allyl bromide under basic conditions. Allylated MC was subsequently crosslinked through UV irradiation in the presence of a photoinitiator for 20 min, at either room temperature or 80 °C, producing two distinct hydrogels, denoted as *xsol*-MC and *xfib*-MC gels respectively, with distinct structures and properties discussed below [122].

The crosslinking of MC using aldehyde groups such as glutaraldehyde (GA) catalyzed by strong acid has been extensively studied as another type of chemical modification [127-130]. In

particular, Rimdusit et al. [130] reported that the swelling ratio and moisture absorption decreased with increasing GA concentration, while the gel content increased and eventually plateaued at higher GA concentrations. In addition, Park et al. [129] revealed that the crosslinking density and tensile strength of the gels increased with increasing GA and acid concentration, while the maximum elongation of the gels decreased. Patenaude et al. [131] demonstrated an alternative way to introduce aldehyde functional groups through the selective oxidation of MC in the presence of sodium periodate at room temperature for 2 h. A subsequent crosslinking reaction with PNIPAm functionalized with hydrazide groups was achieved [131]. Similarly, MC can be functionalized with methacrylate crosslinker groups through esterification of MC hydroxyl groups [148,149]. Stalling et al. [148] showed that methacrylate-modified MC solutions can be crosslinked with a photoinitiator under UV exposure for 10 min at 4 °C [148]. However, Gold et al. [149] argued that the photo crosslinking method restricts clinical applications for *in situ* gelation due to the limited penetrability of UV light into human skin. Instead, an ammonium persulfate-ascorbic acid redox initiation system was utilized to chemically crosslink methacrylate modified MC, in phosphate buffered saline at room temperature [149].

In these chemical crosslinking reactions, MC gels were typically synthesized at or below room temperature [122,125,128-131,148,149], and it was reported that the gels were clear and transparent. Rheological measurements showed that the storage or elastic modulus $G'$ was always greater than $G''$ as a function of time [125], after the onset of gelation [149], and during frequency sweeps and heating ramps [122], as expected for network structures. A common way to tune the hydrogel properties is by changing the MC concentration in the precursor solution [122], whereby increasing the MC concentration decreased the subsequent water uptake, and hence the swelling ratio, while increasing the elastic modulus [122,148,149]. For example, Morozova et al. [122] showed that as the temperature was increased from 25 °C to 80 °C, the equilibrium volume fraction $\phi_e$ for *xsol*-MC gels increased by an order of magnitude due to the gel deswelling. The authors argued that $G'$ in *xsol*-MC arose from the loss in conformational entropy of individual polymer chains as a result of deformation, consistent with established theories for crosslinked polymer chains [122].

The fibril formation behavior of aqueous MC solutions upon heating, concurrent with the onset of gelation and phase separation, has only been known over the past 10 years [43-45], and therefore work on chemically crosslinking MC fibrils has been limited [122]. By chemically crosslinking at 80 °C, opaque and solid *xfib*-MC gels were formed and the opacity persisted even after cooling to room temperature. This indicated the locking in of the fibril structure, as also deduced from SAXS patterns, with the mean fibril radius systematically increasing from 10 to 20 nm upon cooling due to weakening polymer–polymer interactions [122]. On the other hand, crosslinking MC solutions at room temperature was found to prevent fibril formation on subsequent heating [122].

Similar to *xsol*-MC gels, *xfib*-MC gels showed no frequency dependence to the moduli, and $G'$ was larger than $G''$ [122]. $\phi_e$ of *xfib*-MC gels only increased by 50% upon heating to 80 °C, in contrast to the order of magnitude changes for *xsol*-MC gels, attributed to the difference in the swelling mechanism [122]. Additionally, at 80 °C, the scaling of $G'$ with volume fraction for *xfib*-MC gels was similar to that of uncrosslinked MC fibril gels, indicating that the bulk elasticity arose, at least partly, from the bending modulus of the MC fibrils [122].

### 4.5. Outstanding issues

Modification of MC gelation properties is of wide commercial and scientific interest and has been achieved through both the addition of salts to MC aqueous solutions and by chemical modifications through functionalization or chemical crosslinking. These modifications have been recently studied to understand their effect on the MC fibrillar structures.

The addition of salt has been extensively demonstrated to reduce or increase the gelation point of MC solutions. This behavior is now understood in the context of fibrils as well. Besides the effect of the addition of salt on gelation and fibril formation, the diameter of the fibrils decreases monotonically with molar salt concentration. This behavior with salt concentration is unexpected because the fibril morphology is relatively insensitive to variations of most other parameters. This aspect of MC gelation warrants further study.

Grafting different polymers (PEG and PNIPAm) onto the MC backbone has been shown to affect the overall persistence length, fibril diameter, and fibril formation and gelation. Longer polymer grafts and higher grafting densities increase the persistence length and the fibril diameter. At a critical persistence length of 23 nm, the gelation and fibril formation are completely suppressed. This confirms the close correlation between the ability of MC to form fibrils and to gel. Moreover, the solution properties of PNIPAm-grafted MC exhibited an increase in the apparent theta temperature, which implies unfavorable interactions between MC and PNIPAm grafts. Chemical crosslinking of fibrils in the gel state has been shown to preserve the fibrillar structure upon cooling as well. This shows the ability to control gelation through fibril formation, which is potentially of great importance.

Another interesting, yet sparsely studied, modification approach is the chemical attachment of another polymer to MC to form a block copolymer, which permits manipulation of the solution structure and properties. This can potentially broaden the number of applications through microphase separation, and formation of different morphologies as a function of temperature.

## 5. Summary

MC is a highly-studied and well-known polymer with myriad commercial applications as a consequence of its water solubility and gelation properties. Yet, interesting fundamental questions remain about the solution and gel properties of MC. This polymer exhibits LCST behavior in water, with $T_\theta \approx 48$ °C, and gels upon heating. Early studies related MC gelation to hydrophobic attractions, leading to physical crosslinks. More recent experimental results have brought a new understanding concerning the source of gelation. The use of a powerful combination of experimental tools, i.e., cryo-TEM, SANS/SAXS, and rheology, allowed researchers to correlate the gelation of MC with the formation of stiff fibrils, which percolate into a fibrillar network. Experimental work showed that the fibrils consist of both semicrystalline and amorphous domains, with an average water content of 60% by volume. Upon heating, MC spontaneously self-assembles into fibrils with a constant mean diameter that is independent of the MC concentration, the temperature of gelation, and the MC molecular weight. However, it has been found that the fibril contour length and gel strength are both functions of the molecular weight, whereby lower molecular weight polymers form shorter fibrils that result in a less interconnected gel network, as characterized by a lower storage modulus. Furthermore, dilute MC solutions exhibit aggregation and fibril formation behavior when annealed for a prolonged time below $T_\theta$, where water is considered a good solvent, which conflicts with expectations based on Flory-Huggins theory. Along with experimental work, computational modeling has been directed at addressing the fibrillar structure, dimensions, and formation mechanism. However, to date the proposed models fail to account for the key experimental observations. Therefore, the fundamental questions regarding the origin of the reproducible fibril diameter and

the self-assembly mechanism await further experimental and computational efforts. Of particular significance is the issue of fibril nucleation. Primary nucleation may involve formation of small crystalline moieties, recently shown to be present in the fibrillar gel. This could be followed by coalescence of the associated chains, with additional crystallization, leading to the extended fibrils. Conversely, initial fibril formation may involve a predominantly amorphous assembly of MC chains, with the fixed diameter governed by wrapping of helical segments around the periphery, followed by partial crystallization. These represent two possible nucleation mechanisms for a single fibril. Growth of a dense array of fibrils following nucleation, including branching, presents additional puzzles that need to be addressed, although presumably branching reflects participation of sections of a given chain in two or more fibril nuclei. Experimental tools such as liquid-cell TEM may provide in-situ information about the fibril formation process upon heating. Moreover, future computational efforts will benefit from taking into consideration all the recent experimental evidence.

Further studies indicate that the gelation, fibril formation and structure, and gel mechanical properties can be modified through chemical modification, the addition of both salting-in and salting-out salts, and chemical crosslinking. Specifically, grafting of the MC backbone with PEG chains increases the fibril diameter by increasing the persistence length of the polymer, and at high grafting densities completely suppresses fibril formation and gelation. This provides experimental support to the idea that the fibril diameter is controlled by the persistence length of MC. The introduction of salts into MC solutions has been shown to affect the gelation temperature, depending on the salt type. Moreover, recent studies report that an increase in the salt concentration leads to a smaller fibril diameter, while not affecting the semicrystalline structure, regardless of the type of the salt used. This indicates that the diameter is mainly controlled by the amorphous domains in the fibrils. Chemical crosslinking of aqueous MC solutions at different temperatures/states reveals significant changes in the mechanical properties of the systems. These recent findings demonstrate the ability to control the fibril formation, gelation, and mechanical properties of aqueous MC solutions, and may potentially expand the variety of applications of MC. Another important and not well-explored route is the synthesis of MC-derived block copolymers. Such polymers may form interesting micro-phase separated structures upon heating, which could further broaden MC industrial use.

In summary, MC is an extraordinarily versatile macromolecular platform with many documented structural features, physical properties, and uses. Despite substantial recent advances in understanding, the detailed mechanism of fibril nucleation and growth, and the appropriate thermodynamic and structural models, remain elusive. We speculate that deeper understanding will expose undiscovered opportunities for further development.

## Declaration of Competing Interest

The authors declare that they have no known competing financial interests or personal relationships that could have appeared to influence the work reported in this paper.

## CRediT authorship contribution statement

**McKenzie L. Coughlin:** Visualization, Writing - original draft, Writing - review & editing. **Lucy Liberman:** Visualization, Writing - original draft, Writing - review & editing. **S. Piril Ertem:** Writing - original draft. **Jerrick Edmund:** Writing - original draft. **Frank S. Bates:** Supervision, Writing - review & editing. **Timothy P. Lodge:** Conceptualization, Supervision, Writing - review & editing.

## Acknowledgments

This work was supported primarily by the National Science Foundation through the University of Minnesota MRSEC under Award Numbers DMR-1420013 and DMR-2011401. We acknowledge illuminating discussions with V. Ginzburg, R. Sammler, and K. Dorfman.

## References

[1] Anonymous. US food and drug administration GRAS substances (SCOGS) database. http://www.fda.gov/food/ingredientspackaginglabeling/gras/scogs/ 2018;accessed Jun 2020.
[2] Denham WS, Woodhouse H. CLXXXVI.—the methylation of cellulose. J Chem Soc, Trans 1913;103:1735–42.
[3] Lilienfeld L. Alkyl ethers of cellulose and process of making the same. US-1188376-A, 1916.
[4] Haque A, Morris ER. Thermogelation of methylcellulose. Part I: molecular structures and processes. Carbohydr Polym 1993;22:161–73.
[5] Chatterjee T, Nakatani AI, Adden R, Brackhagen M, Redwine D, Shen H, Li Y, Wilson T, Sammler RL. Structure and properties of aqueous methylcellulose gels by small-angle neutron scattering. Biomacromolecules 2012;13:3355–69.
[6] Reibert KC, Conklin JR. Cellulose ether having enhanced gel strength and compositions containing it. US-6228416-B1, 2001.
[7] Nasatto PL, Pignon F, Silveira JLM, Duarte MER, Noseda MD, Rinaudo M. Methylcellulose, a cellulose derivative with original physical properties and extended applications. Polymers 2015;7:777–803.
[8] Schuyten HA, Weaver JW, Reid JD, Jurgens JF. Trimethylsilylcellulose. J Am Chem Soc 1948;70:1919–20.
[9] Sarkar N. Thermal gelation properties of methyl and hydroxypropyl methylcellulose. J Appl Polym Sci 1979;24:1073–87.
[10] Takahashi M, Shimazaki M, Yamamoto J. Thermoreversible gelation and phase separation in aqueous methyl cellulose solutions. J Polym Sci Part B Polym Phys 2001;39:91–100.
[11] Chevillard C, Axelos MAV. Phase separation of aqueous solution of methylcellulose. Colloid Polym Sci 1997;275:537–45.
[12] Arvidson SA, Lott JR, McAllister JW, Zhang J, Bates FS, Lodge TP, Sammler RL, Li Y, Brackhagen M. Interplay of phase separation and thermoreversible gelation in aqueous methylcellulose solutions. Macromolecules 2013;46:300–9.
[13] Fairclough JPA, Yu H, Kelly O, Ryan AJ, Sammler RL, Radler M. Interplay between gelation and phase separation in aqueous solutions of methylcellulose and hydroxypropylmethylcellulose. Langmuir 2012;28:10551–7.
[14] Kobayashi K, Huang CI, Lodge TP. Thermoreversibe gelation of methylcellulose solutions. Macromolecules 1999;32:7070–7.
[15] Desbrières J, Hirrien M, Ross-Murphy SB. Thermogelation of methylcellulose: rheological considerations. Polymer 2000;41:2451–61.
[16] Li L, Thangamathesvaran PM, Yue CY, Tam KC, Hu X, Lam YC. Gel network structure of methylcellulose in water. Langmuir 2001;17:8062–8.
[17] Savage AB. Temperature-viscosity relationships for water-soluble cellulose ethers. Ind Eng Chem 1957;49:99–103.
[18] McAllister JW, Schmidt PW, Dorfman KD, Lodge TP, Bates FS. Thermodynamics of aqueous methylcellulose solutions. Macromolecules 2015;48:7205–15.
[19] Heymann E. Studies on sol-gel transformations I. The inverse sol-gel transformation of methylcellulose in water. Trans Faraday Soc 1935;31:846–64.
[20] Nishinari K, Hofmann KE, Moritaka H, Kohyama K, Nishinari N. Gel-sol transition of methylcellulose. Macromol Chem Phys 1997;198:1217–26.
[21] Wang Q, Li L. Effects of molecular weight on thermoreversible gelation and gel elasticity of methylcellulose in aqueous solution. Carbohydr Polym 2005;62:232–8.
[22] Schmidt PW, Morozova S, Owens PM, Adden R, Li Y, Bates FS, Lodge TP. Molecular weight dependence of methylcellulose fibrillar networks. Macromolecules 2018;51:7767–75.
[23] Erler U, Mischnick P, Stein A, Klemm D. Determination of the substitution patterns of cellulose methyl ethers by HPLC and GLC-comparison of methods. Polym Bull 1992;29:349–56.
[24] Saake B, Lebioda S, Puls J. Analysis of the substituent distribution along the chain of water-soluble methyl cellulose by combination of enzymatic and chemical methods. Holzforschung 2004;58:97–104.
[25] Desbrières J, Hirrien M, Rinaudo M. Relation between the conditions of modification and the properties of cellulose derivatives: thermogelation of methylcellulose. ACS Symp Ser 1998;688:332–48.
[26] Ibbett RN, Philp K, Price DM. 13C N.M.R. studies of the thermal behaviour of aqueous solutions of cellulose ethers. Polymer 1992;33:4087–94.
[27] Hirrien M, Chevillard C, Desbrières J, Axelos MAV, Rinaudo M. Thermogelation of methylcelluloses: new evidence for understanding the gelation mechanism. Polymer 1998;39:6251–9.
[28] Kono H, Fujita S, Tajima K. NMR characterization of methylcellulose: chemical shift assignment and mole fraction of monomers in the polymer chains. Carbohydr Polym 2017;157:728–38.
[29] Sarkar N. Kinetics of thermal gelation of methylcellulose and hydroxypropylmethylcellulose in aqueous solutions. Carbohydr Polym 1995;26:195–203.

[30] Kato T, Yokoyama M, Takahashi A. Melting temperatures of thermally reversible gels IV. Methyl cellulose-water gels. Colloid Polym Sci 1978;256:15–21.
[31] Khomutov LI, Ryskina II, Panina NI, Dubina LG, Timofeeva GN. Structural changes during gelation of aqueous solutions of methylcellulose. Polym Sci 1993;35:320–3.
[32] Rees DA. Polysaccharide gels: a molecular view. Chem Ind 1972;19:630–6.
[33] Takahashi M, Shimazaki M. Formation of junction zones in thermoreversible methylcellulose gels. J Polym Sci Part B Polym Phys 2001;39:943–6.
[34] Takeshita H, Saito K, Miya M, Takenaka K, Shiomi T. Laser speckle analysis on correlation between gelation and phase separation in aqueous methyl cellulose solutions. J Polym Sci Part B Polym Phys 2010;48:168–74.
[35] Villetti MA, Soldi V, Rochas C, Borsali R. Phase-separation kinetics and mechanism in a methylcellulose/salt aqueous solution studied by time-resolved small-angle light scattering (SALS). Macromol Chem Phys 2011;212:1063–71.
[36] Rosell KG. Distribution of substituents in methylcellulose. J Carbohydr Chem 1988;7:525–36.
[37] Tezuka Y, Imai K, Oshima M, Chiba T. Determination of substituent distribution in cellulose ethers by means of a 13C NMR study on their acetylated derivatives. 1. Methylcellulose. Macromolecules 1987;20:2413–18.
[38] Tanaka F, Ishida M. Thermoreversible gelation of hydrated polymers. J Chem Soc Faraday Trans 1995;91:2663–70.
[39] Tanaka F, Ishida M. Elastically effective chains in transient gels with multiple junctions. Macromolecules 1996;29:7571–80.
[40] Tanaka F, Nishinari K. Junction multiplicity in thermoreversible gelation. Macromolecules 1996;29:3625–8.
[41] Tanaka F. Thermoreversible gelation strongly coupled to polymer conformational transition. Macromolecules 2000;33:4249–63.
[42] Tanaka H. Viscoelastic phase separation. J Phys Condens Matter 2000;12:R207–64.
[43] Bodvik R, Dedinaite A, Karlson L, Bergström M, Bäverbäck P, Pedersen JS, Edwards K, Karlsson G, Varga I, Claesson PM. Aggregation and network formation of aqueous methylcellulose and hydroxypropylmethylcellulose solutions. Colloids Surf A 2010;354:162–71.
[44] Lott JR, McAllister JW, Arvidson SA, Bates FS, Lodge TP. Fibrillar structure of methylcellulose hydrogels. Biomacromolecules 2013;14:2484–8.
[45] Lott JR, McAllister JW, Wasbrough M, Sammler RL, Bates FS, Lodge TP. Fibrillar structure in aqueous methylcellulose solutions and gels. Macromolecules 2013;46:9760–71.
[46] Chen WR, Butler PD, Magid LJ. Incorporating intermicellar interactions in the fitting of SANS data from cationic wormlike micelles. Langmuir 2006;22:6539–48.
[47] Pedersen JS, Schurtenberger P. Scattering functions of semiflexible polymers with and without excluded volume effects. Macromolecules 1996;29:7602–12.
[48] Huang W, Ramesh R, Jha PK, Larson RG. A systematic coarse-grained model for methylcellulose polymers: spontaneous ring formation at elevated temperature. Macromolecules 2016;49:1490–503.
[49] Huang W, Huang M, Lei Q, Larson RG. A simple analytical model for predicting the collapsed state of self-attractive semiflexible polymers. Polymers 2016;8:264.
[50] Ginzburg VV, Sammler RL, Huang W, Larson RG. Anisotropic self-assembly and gelation in aqueous methylcellulose—theory and modeling. J Polym Sci Part B Polym Phys 2016;54:1624–36.
[51] Li X, Bates FS, Dorfman KD. Rapid conformational fluctuations in a model of methylcellulose. Phys Rev Mater 2017;1:025604.
[52] Sethuraman V, Dorfman KD. Simulating precursor steps for fibril formation in methylcellulose solutions. Phys Rev Mater 2019;3:55601.
[53] Hall DM, Bruss IR, Barone JR, Grason GM. Morphology selection via geometric frustration in chiral filament bundles. Nat Mater 2016;15:727–32.
[54] Schmidt PW, Morozova S, Ertem SP, Coughlin ML, Davidovich I, Talmon Y, Reineke TM, Bates FS, Lodge TP. Internal structure of methylcellulose fibrils. Macromolecules 2020;53:398–405.
[55] Morozova S, Schmidt PW, Bates FS, Lodge TP. Effect of poly(ethylene glycol) grafting density on methylcellulose fibril formation. Macromolecules 2018;51:9413–21.
[56] Vargas-Lara F, Douglas J. Fiber network formation in semi-flexible polymer solutions: an exploratory computational study. Gels 2018;4:27.
[57] Morozova S. Methylcellulose fibrils: a mini review. Polym Int 2020;69:125–30.
[58] Hall DM, Grason GM. How geometric frustration shapes twisted fibres, inside and out: competing morphologies of chiral filament assembly. Interface Focus 2017;7:20160140.
[59] Paavilainen S, Róg T, Vattulainen I. Analysis of twisting of cellulose nanofibrils in atomistic molecular dynamics simulations. J Phys Chem B 2011;115:3747–55.
[60] Grason GM, Bruinsma RF. Chirality and equilibrium biopolymer bundles. Phys Rev Lett 2007;99:098101.
[61] Grason GM. Braided bundles and compact coils: the structure and thermodynamics of hexagonally packed chiral filament assemblies. Phys Rev E 2009;041919:1–15 79.
[62] Bruss IR, Grason GM. Topological defects, surface geometry and cohesive energy of twisted filament bundles. Soft Matter 2013;9:8327–45.
[63] Schmidt PW. Fibrillar structure and networks in methylcellulose hydrogels. University of Minnesota; 2018. p. 132. PhD Thesis.
[64] Nishiyama Y, Langan P, Chanzy H. Crystal structure and hydrogen-bonding system in cellulose I$\beta$ from synchrotron X-ray and neutron fiber diffraction. J Am Chem Soc 2002;124:9074–82.
[65] Zugenmaier P, Kuppel A. Diffraction studies on trimethylcellulose and trimethylmannan. Colloid Polym Sci 1986;264:231–5.
[66] Nishiyama Y, Sugiyama J, Chanzy H, Langan P. Crystal structure and hydrogen bonding system in cellulose I$\alpha$ from synchrotron X-ray and neutron fiber diffraction. J Am Chem Soc 2003;125:14300–6.
[67] Rubinstein M, Colby RH. Polymer physics. New York: Oxford University Press; 2003. p. 448.
[68] Flory PJ. Statistical thermodynamics of semi-flexible chain molecules. Proc R Soc London Ser A 1956;234:60–73.
[69] McAllister JW, Lott JR, Schmidt PW, Sammler RL, Bates FS, Lodge TP. Linear and nonlinear rheological behavior of fibrillar methylcellulose hydrogels. ACS Macro Lett 2015;4:538–42.
[70] Mackintosh FC, Kas J, Janmey PA. Elasticity of semi-flexible biopolymer networks. Phys Rev Lett 1995;75:4425–8.
[71] Morozova S, Schmidt PW, Metaxas A, Bates FS, Lodge TP, Dutcher CS. Extensional flow behavior of methylcellulose solutions containing fibrils. ACS Macro Lett 2018;7:347–52.
[72] Micklavzina BL, Metaxas AE, Dutcher CS. Microfluidic rheology of methylcellulose solutions in hyperbolic contractions and the effect of salt in shear and extensional flows. Soft Matter 2020;16:5273–81.
[73] Metaxas AE, Coughlin ML, Clayton CK, Bates FS, Lodge TP, Dutcher CS. Microfluidic filament thinning of aqueous, fibrillar methylcellulose solutions. Phys Rev Fluids 2020;5:113302.
[74] Arbeiten aus dem Pharmakologischen Institut der Deutschen Universität zu Prag. 12zur lehre von der wirkung der salze. dritte mittheilung. Arch Exp Pathol Pharmakol 1888;25:1–30.
[75] Dougherty RC. Density of salt solutions: effect of ions on the apparent density of water. J Phys Chem B 2001;105:4514–19.
[76] dos Santos AP, Diehl A, Levin Y. Surface tensions, surface potentials, and the Hofmeister series of electrolyte solutions. Langmuir 2010;26:10778–83.
[77] Xu Y, Wang C, Tam KC, Li L. Salt-assisted and salt-suppressed sol-gel transitions of methylcellulose in water. Langmuir 2004;20:646–52.
[78] Almeida N, Rakesh L, Zhao J. The effect of kappa carrageenan and salt on thermoreversible gelation of methylcellulose. Polym Bull 2018;75:4227–43.
[79] Xu Y, Li L, Zheng P, Lam YC, Hu X. Controllable gelation of methylcellulose by a salt mixture. Langmuir 2004;20:6134–8.
[80] Shibata M, Koga T, Nishida K. Effect of organic anion with multiple hydrophobic sites on gelation and phase separation in aqueous methylcellulose solution: beyond simple salting-in effect. Polymer 2019;178:121574.
[81] Nishida K, Morita H, Katayama Y, Inoue R, Kanaya T, Sadakane K, Seto H. Salting-out and salting-in effects of amphiphilic salt on cloud point of aqueous methylcellulose. Process Biochem 2017;59:52–7.
[82] Liberman L, Schmidt PW, Coughlin ML, Matatyaho A, Davidovich I, Edmund J, Ertem SP, Morozova S, Talmon Y, Bates FS, Lodge TP. Salt dependent structure in methylcellulose fibrillar gels. Macromolecules under review
[83] Schorger AW, Shoemaker MJ. Hydroxyalkyl ethers of cellulose. Ind Eng Chem 1937;29:114–17.
[84] Kamide K. Cellulose and Cellulose Derivatives: Molecular Characterization and Its Applications. Amsterdam: Elsevier Science & Technology; 2005. p. 652.
[85] Sebti I, Delves-Broughton J, Coma V. Physicochemical properties and bioactivity of nisin-containing cross-linked hydroxypropylmethylcellulose films. J Agric Food Chem 2003;51:6468–74.
[86] Pérez OE, Sánchez CC, Rodríguez Patino JM, Pilosof AMR. Thermodynamic and dynamic characteristics of hydroxypropylmethylcellulose adsorbed films at the air-water interface. Biomacromolecules 2006;7:388–93.
[87] Bilbao-Sáinz C, Avena-Bustillos RJ, Wood DF, Williams TG, McHugh TH. Composite edible films based on hydroxypropyl methylcellulose reinforced with microcrystalline cellulose nanoparticles. J Agric Food Chem 2010;58:3753–60.
[88] Otoni CG, Lorevice MV, de Moura MR, Mattoso LHC. On the effects of hydroxyl substitution degree and molecular weight on mechanical and water barrier properties of hydroxypropyl methylcellulose films. Carbohydr Polym 2018;185:105–11.
[89] Zhang J, Schneiderman DK, Li T, Hillmyer MA, Bates FS. Design of graft block polymer thermoplastics. Macromolecules 2016;49:9108–18.
[90] Zhang J, Li T, Mannion AM, Schneiderman DK, Hillmyer MA, Bates FS. Tough and sustainable graft block copolymer thermoplastics. ACS Macro Lett 2016;5:407–12.
[91] Long Y, Zhao X, Liu S, Chen M, Liu B, Ge J, Jia YG, Ren L. Collagen–hydroxypropyl methylcellulose membranes for corneal regeneration. ACS Omega 2018;3:1269–75.
[92] Viridén A, Wittgren B, Larsson A. Investigation of critical polymer properties for polymer release and swelling of HPMC matrix tablets. Eur J Pharm Sci 2009;36:297–309.
[93] Williams HD, Ward R, Hardy IJ, Melia CD. The effect of sucrose and salts in combination on the drug release behaviour of an HPMC matrix. Eur J Pharm Biopharm 2010;76:433–6.
[94] Bhowmik M, Das S, Chattopadhyay D, Ghosh LK. Study of thermo-sensitive in-situ gels for ocular delivery. Sci Pharm 2011;79:351–8.
[95] Zhou D, Law D, Reynolds J, Davis L, Smith C, Torres JL, Dave V, Gopinathan N, Hernandez DT, Springman MK, et al. Understanding and managing the impact of HPMC variability on drug release from controlled release formulations. J Pharm Sci 2014;103:1664–72.

[96] Ali L, Ahmad M, Usman M. Evaluation of cross-linked hydroxypropyl methylcellulose graft-methacrylic acid copolymer as extended release oral drug carrier. Cellul Chem Technol 2015;49:143–51.
[97] Liu S, Jia L, Xu S, Chen Y, Tang W, Gong J. Insight into the state evolution of norfloxacin as a function of drug concentration in norfloxacin-vinylpyrrolidone/hydroxypropyl methylcellulose/hydroxypropyl methylcellulose phthalate solid dispersions. Cryst Growth Des 2019;19:6239–51.
[98] Mitchell K, Ford JL, Armstrong DJ, Elliott PNC, Hogan JE, Rostron C. The influence of substitution type on the performance of methylcellulose and hydroxypropylmethycellulose in gels and matrices. Int J Pharm 1993;100:143–54.
[99] Polamaplly P, Cheng Y, Shi X, Manikandan K, Zhang X, Kremer GE, Qin H. 3D printing and characterization of hydroxypropyl methylcellulose and methylcellulose for biodegradable support structures. Polymer 2019;173:119–26.
[100] Lodge TP, Maxwell AL, Lott JR, Schmidt PW, McAllister JW, Morozova S, Bates FS, Li Y, Sammler RL. Gelation, phase separation, and fibril formation in aqueous hydroxypropylmethylcellulose solutions. Biomacromolecules 2018;19:816–24.
[101] Bodvik R, Karlson L, Edwards K, Eriksson J, Thormann E, Claesson PM. Aggregation of modified celluloses in aqueous solution: transition from methylcellulose to hydroxypropylmethylcellulose solution properties induced by a low-molecular-weight oxyethylene additive. Langmuir 2012;28:13562–9.
[102] Haque A, Richardson RK, Morris ER, Gidley MJ, Caswell DC. Thermogelation of methylcellulose. Part II: effect of hydroxypropyl substituents. Carbohydr Polym 1993;22:175–86.
[103] Kita R, Kaku T, Kubota K, Dobashi T. Pinning of phase separation of aqueous solution of hydroxypropylmethylcellulose by gelation. Phys Lett Sect A 1999;259:302–7.
[104] Hussain S, Keary C, Craig DQM. A thermorheological investigation into the gelation and phase separation of hydroxypropyl methylcellulose aqueous systems. Polymer 2002;43:5623–8.
[105] Viridén A, Wittgren B, Andersson T, Abrahmsén-Alami S, Larsson A. Influence of substitution pattern on solution behavior of hydroxypropyl methylcellulose. Biomacromolecules 2009;10:522–9.
[106] Akinosho H, Hawkins S, Wicker L. Hydroxypropyl methylcellulose substituent analysis and rheological properties. Carbohydr Polym 2013;98:276–81.
[107] Shahin A, Nicolai T, Benyahia L, Tassin JF, Chassenieux C. Evidence for the coexistence of interpenetrating permanent and transient networks of hydroxypropyl methyl cellulose. Biomacromolecules 2014;15:311–18.
[108] Arai K, Horikawa Y, Shikata T, Iwase H. Reconsideration of the conformation of methyl cellulose and hydroxypropyl methyl cellulose ethers in aqueous solution. RSC Adv 2020;10:19059–66.
[109] Klug ED. Some properties of water-soluble hydroxyalkyl celluloses and their derivatives. J Polym Sci Part C Polym Symp 1971;508:491–508.
[110] Guido S. Phase behavior of aqueous solutions of hydroxypropylcellulose. Macromolecules 1995;28:4530–9.
[111] Gao J, Haidar G, Lu X, Hu Z. Self-association of hydroxypropylcellulose in water. Macromolecules 2001;34:2242–7.
[112] Carotenuto C, Grizzuti N. Thermoreversible gelation of hydroxypropylcellulose aqueous solutions. Rheol Acta 2006;45:468–73.
[113] Jing Y, Wu P. Study on the thermoresponsive two phase transition processes of hydroxypropyl cellulose concentrated aqueous solution: from a microscopic perspective. Cellulose 2013;20:67–81.
[114] Koch W. Properties and uses of ethylcellulose. Ind Eng Chem 1937;29:687–90.
[115] Jullander I. Water-soluble ethylhydroxyethylcellulose. Ind Eng Chem 1957;49:364–8.
[116] Benchabane A, Bekkour K. Rheological properties of carboxymethyl cellulose (CMC) solutions. Colloid Polym Sci 2008;286:1173–80.
[117] Bekkour K, Sun-Waterhouse D, Wadhwa SS. Rheological properties and cloud point of aqueous carboxymethyl cellulose dispersions as modified by high or low methoxyl pectin. Food Res Int 2014;66:247–56.
[118] Barros SC, Silva MM. Seeking the lowest phase transition temperature in a cellulosic system for textile applications. Cellulose 2018;25:3163–78.
[119] Quiñones JP, Mardare CC, Hassel AW, Brüggemann O. Testosterone- and vitamin-grafted cellulose ethers for sustained release of camptothecin. Carbohydr Polym 2019;206:641–52.
[120] Dong Y, Mosquera-Giraldo LI, Taylor LS, Edgar KJ. Amphiphilic cellulose ethers designed for amorphous solid dispersion via olefin cross-metathesis. Biomacromolecules 2016;17:454–65.
[121] Dong Y, Mosquera-Giraldo LI, Taylor LS, Edgar KJ. Tandem modification of amphiphilic cellulose ethers for amorphous solid dispersion via olefin cross-metathesis and thiol-michael addition. Polym Chem 2017;8:3129–39.
[122] Morozova S, Coughlin ML, Early JT, Ertem SP, Reineke TM, Bates FS, Lodge TP. Properties of chemically cross-linked methylcellulose gels. Macromolecules 2019;52:7740–8.
[123] Morozova S, Lodge TP. Conformation of methylcellulose as a function of poly(ethylene glycol) graft density. ACS Macro Lett 2017;6:1274–9.
[124] Shin JY, Yeo YH, Jeong JE, Park SA, Park WH. Dual-crosslinked methylcellulose hydrogels for 3D bioprinting applications. Carbohydr Polym 2020;238:116192.
[125] Pakulska MM, Vulic K, Tam RY, Shoichet MS. Hybrid crosslinked methylcellulose hydrogel: a predictable and tunable platform for local drug delivery. Adv Mater 2015;27:5002–8.
[126] Hatakeyama H, Onishi T, Endo T, Hatakeyama T. Gelation of chemically cross-linked methylcellulose studied by DSC and AFM. Carbohydr Polym 2007;69:792–8.
[127] Rokhade AP, Shelke NB, Patil SA, Aminabhavi TM. Novel Interpenetrating polymer network microspheres of chitosan and methylcellulose for controlled release of theophylline. Carbohydr Polym 2007;69:678–87.
[128] Park JS, Ruckenstein E. Viscoelastic properties of plasticized methylcellulose and chemically crosslinked methylcellulose. Carbohydr Polym 2001;46:373–81.
[129] Rimdusit S, Somsaeng K, Kewsuwan P, Jubsilp C, Tiptipakorn S. Comparison of gamma radiation crosslinking and chemical crosslinking on properties of methylcellulose hydrogel. Eng J 2012;16:15–28.
[130] Park JS, Park JW, Ruckenstein E. Thermal and dynamic mechanical analysis of PVA/MC blend hydrogels. Polymer 2001;42:4271–80.
[131] Patenaude M, Hoare T. Injectable mixed natural-synthetic polymer hydrogels with modular properties. Biomacromolecules 2012;13:369–78.
[132] Kim K, Ryu K, Kim T. Cationic methylcellulose derivative with serum-compatibility and endosome buffering ability for gene delivery systems. Carbohydr Polym 2014;110:268–77.
[133] Fredrickson GH. Surfactant-induced lyotropic behavior of flexible polymer solutions. Macromolecules 1993;26:2825–31.
[134] Steiert E, Konhäuser M, Wang Y, Breitenbach BB, Parekh SH, Wich PR, Vogt LM. Double stimuli-responsive polysaccharide block copolymers as green macrosurfactants for near-infrared photodynamic therapy. Soft Matter 2019;15:1423–34.
[135] Breitenbach BB, Schmid I, Wich PR. Amphiphilic polysaccharide block copolymers for pH-responsive micellar nanoparticles. Biomacromolecules 2017;18:2839–48.
[136] Schatz C, Lecommandoux S. Polysaccharide-containing block copolymers: synthesis, properties and applications of an emerging family of glycoconjugates. Macromol Rapid Commun 2010;31:1664–84.
[137] Novoa-Carballal R, Müller AHE. Synthesis of polysaccharide-b-PEG block copolymers by oxime click. Chem Commun 2012;48:3781–3.
[138] Dax D, Xu C, Långvik O, Hemming J, Backman P, Willför S. Synthesis of SET-LRP-induced galactoglucomannan-diblock copolymers. J Polym Sci Part A Polym Chem 2013;51:5100–10.
[139] Lin F, Cousin F, Putaux JL, Jean B. Temperature-controlled star-shaped cellulose nanocrystal assemblies resulting from asymmetric polymer grafting. ACS Macro Lett 2019;8:345–51.
[140] Enomoto-Rogers Y, Iwata T. Syntheses of poly(L-Lactide)-block-xylan butyrate-block-poly(L-Lactide) triblock copolymers and their properties. J Wood Sci 2013;59:489–98.
[141] Wang J, Caceres M, Li S, Deratani A. Synthesis and self-assembly of amphiphilic block copolymers from biobased hydroxypropyl methyl cellulose and poly(L-Lactide). Macromol Chem Phys 2017;218:1600558.
[142] Kamitakahara H, Enomoto Y, Hasegawa C, Nakatsubo F. Synthesis of diblock copolymers with cellulose derivatives. 2. Characterization and thermal properties of cellulose triacetate-block-oligoamide-15. Cellulose 2005;12:527–41.
[143] Kamitakahara H, Nakatsubo F, Klemm D. Block co-cligomers of tri-O-methylated and unmodified cello-oligosaccharides as model compounds for methylcellulose and its dissolution/gelation behavior. Cellulose 2006;13:375–92.
[144] Nakagawa A, Fenn D, Koschella A, Heinze T, Kamitakahara H. Synthesis of diblock methylcellulose derivatives with regioselective functionalization patterns. J Polym Sci Part A Polym Chem 2011;49:4964–76.
[145] Nakagawa A, Kamitakahara H, Takano T. Synthesis and thermoreversible gelation of diblock methylcellulose analogues via huisgen 1,3-dipolar cycloaddition. Cellulose 2012;19:1315–26.
[146] Kamitakahara H, Suhara R, Yamagami M, Kawano H, Okanishi R, Asahi T, Takano T. A versatile pathway to end-functionalized cellulose ethers for click chemistry applications. Carbohydr Polym 2016;151:88–95.
[147] Chen J, Kamitakahara H, Edgar KJ. Synthesis of polysaccharide-based block copolymers via olefin cross-metathesis. Carbohydr Polym 2020;229:115530.
[148] Stalling SS, Akintoye SO, Nicoll SB. Development of photocrosslinked methylcellulose hydrogels for soft tissue reconstruction. Acta Biomater 2009;5:1911–18.
[149] Gold GT, Varma DM, Taub PJ, Nicoll SB. Development of crosslinked methylcellulose hydrogels for soft tissue augmentation using an ammonium persulfate-ascorbic acid redox system. Carbohydr Polym 2015;134:497–507.